



THESIS APPROVAL
GRADUATE SCHOOL, KASETSART UNIVERSITY

Master of Science (Chemistry)

DEGREE

Chemistry

Chemistry

FIELD

DEPARTMENT

TITLE: Excitation Energies of Triphenylamine Cyanoacrylic Acid for
Dye-Sensitized Solar Cells Using Long-Range Corrected
Time-Dependent Density Functional Theory

NAME: Mr. Chirawat Chitpakdee

THIS THE SIS HAS BEEN ACCEPTED BY

THESIS ADVISOR

(Mr. Songwut Suramitr, Ph.D.)

THESIS CO-ADVISOR

(Associate Professor Supa Hannongbua, Dr.rer.nat.)

THESIS CO-ADVISOR

(Mr. Jakkapan Sirijaraensre, Ph.D.)

DEPARTMENT HEAD

(Associate Professor Supa Hannongbua, Dr.rer.nat.)

APPROVED BY THE GRADUATE SCHOOL ON

DEAN

(Associate Professor Gunjana Theeragool, D.Agr.)

THESIS

EXCITATION ENERGIES OF TRIPHENYLAMINE
CYANOACRYLIC ACID FOR DYE-SENSITIZED SOLAR CELLS
USING LONG-RANGE CORRECTED TIME-DEPENDENT DENSITY
FUNCTIONAL THEORY

CHIRAWAT CHITPAKDEE

A Thesis Submitted in Partial Fulfillment of
the Requirements for the Degree of
Master of Science (Chemistry)
Graduate School, Kasetsart University
2011

Chirawat Chitpakdee 2011: Excitation Energies of Triphenylamine
Cyanoacrylic Acid for Dye-Sensitized Solar Cells Using Long-Range
Corrected Time-Dependent Density Functional Theory. Master of Science
(Chemistry), Major Field: Chemistry, Department of Chemistry.
Thesis Advisor: Mr. Songwut Suramitr, Ph.D. 60 pages.

Structures of 2-cyano-3-(4-(diphenylamino)-phenyl) acrylic acid (TC) and its derivatives were investigated using density functional theory (DFT). The structural parameters were optimized using several DFT functional, B3LYP, M06, M06-HF, M06-L, and M06-2X at 6-31G(d) basis set level. The structures obtained from various methods were used to calculate the electronic properties by TD-B3LYP/6-311G(d,p) in gas phase and compare with the experimental absorption bands. The obtained results indicate that the excitation energy from structure using M06-HF/6-31G(d) method (410 nm) is in well agreement with experimental absorption data (400 nm). Therefore, the optimized structures of TC derivatives obtained from M06-HF/6-31G(d) method are also calculated for the excitation energies using TD-DFT functional, PBE0, LC-B3LYP, LC-wPBE and CAM-B3LYP at 6-311G(d,p) level including conductor polarizable continuum model (PCM) solvation to compare with the experimental absorption bands. The results show that the absorption spectrum using the state-specific polarizable continuum model (SS-PCM) SS-PCM-TD-CAM-B3LYP/6-311G(d,p) methods (393 nm) are closer to experimental absorption data (400 nm). We conclude by discussing the benefits of theoretical calculations, which can provide critical structural and electronic understanding of electron transfer phenomena that can be exploited in design of novel optical materials.

Student's signature

Thesis Advisor's signature

ACKNOWLEDGEMENTS

I sincerely thank my advisor, Dr. Songwut Suramitr for his tremendous support and meticulous attention throughout the duration of my graduate study and research. I also wish to express my appreciation to my advisory committee Assistant Professor Associate Professor Supa Hannongbua and Dr. Jakkapan Sirijaraensre the representative of Graduate School, for their worthy suggestion and constructive criticism.

I would like to express my deep gratitude to the National Center of Excellence in Petroleum, Petrochemical Technology, Center of Nanotechnology Kasetsart University, Kasetsart University Research and Development Institute (KURDI), Laboratory of Computational and Applied Chemistry (LCAC), the Commission on Higher Education via the "National Research University Project of Thailand" (NRU) are sincere thanked for scholarship and research facilities. I would also like to thank all of staffs at Department of Chemistry, Faculty of Science, Kasetsart University for research supportably.

Finally, I wish to thanks my family and friends for their advice, encouragement and understanding.

Chirawat Chitpakdee

May, 2011

TABLE OF CONTENTS

	Page
TABLE OF CONTENTS	i
LIST OF TABLES	ii
LIST OF FIGURES	iv
LIST OF ABBREVIATIONS	vi
INTRODUCTION	1
OBJECTIVES	8
LITERATURE REVIEW	9
MATERIALS AND METHODS	14
RESULTS AND DISCUSSION	18
CONCLUSIONS	39
LITERATURE CITED	40
APPENDICES	45
Appendix A Theoretical Background	46
Appendix B Publication	53
CURRICULUM VITAE	60

LIST OF TABLES

Table		Page
1	Structural parameters of triphenylamine obtained from full optimization using HF, B3LYP and MP2 methods at 6-31G(d) level of basis set (Bond length in angstrom and Angle in degrees). The mean relative error values are also listed.	19
2	Structural parameters of 2-Cyano-3-(4-(diphenylamino)phenyl) acrylic acid obtained from full optimization by B3LYP and M06 functional at 6-31G(d) level of basis set (Bond length in angstrom and Angle in degrees).	22
3	Vertical excitation of TC1 obtained from TD-B3LYP/6-31G(d,p) method in gas phase based on ground state geometries, and the experimental absorption wavelength in the methanol solvent.	23
4	Vertical excitation of TC1 molecule obtained from PCM-TD-DFT methods in methanol at 6-311G(d,p) basis set based on ground state geometries.	25
5	Structural parameters of TC1, TC2, TC3 and TC4 obtained from full optimization by M06-HF functional at 6-31G(d,p) level of basis set (Bond length in angstrom and Angle in degrees).	26
6	Vertical excitation of TC1 molecule obtained from TD-CAM-B3LYP/6-311G(d,p) that was calculated in gas phase and various PCM methods.	27
7	Vertical excitation of TC1 molecule obtained from several SS-PCM-TD-DFT methods in methanol at 6-311G(d,p) basis set based on ground state geometries and experiment data.	29

LIST OF TABLES (Continued)

Table		Page
8	Vertical excitation of triphenylamine cyanoacrylic acid derivative (TC1-TC4) obtained from TD-CAM-B3LYP/6-311G(d,p) that was calculated in SS-PCM methods, compared with maximum absorbance from experimental data.	31
9	Ionization potential (IP) and electron affinity (EA), calculated at M06-HF/6-31G(d), compared with percent conversion efficiency from experimental data.	36

LIST OF FIGURES

Figure		Page
1	Generating electricity of P-N junction solar cell.	2
2	Components and electron flow of dye-sensitized solar cells (DSSCs).	3
3	Structure of Ru complexes dye (a) N3, (b) N179 and (c) black dye.	4
4	Molecular structures of triphenylamine cyanoacrylic acid.	5
5	Molecular structures based on triphenylamine (TPA) moieties as the donor and cyanoacetic acid moieties as the electron acceptor groups by Xu <i>et al.</i> (2008).	6
6	Synthesis rout of 2-cyano-3-(4-(diphenylamino)-phenyl) acrylic acid (TC1).	14
7	Conformation of Triphenylamine and atom numbering scheme.	18
8	Bond lengths of triphnylamine obtained from various methods are compared with X-ray data.	20
9	Bond angle of triphnylamine obtained from various methods are compared with X-ray data.	20
10	Equilibrium structure of 2-Cyano-3-(4-(diphenylamino)phenyl) acrylic Acid (TC1).	21
11	Electronic density of frontier orbitals of TC1 molecule.	30
12	Electronic density of frontier orbitals of TC2 molecule.	33
13	Electronic density of frontier orbitals of TC3 molecule.	34
14	Electronic density of frontier orbitals of TC4 molecule.	35
15	¹ H-NMR spectrum of 2-cyano-3-(4-(diphenylamino)-phenyl) acrylic acid.	37
16	Absorption spectra of 2-cyano-3-(4-(diphenylamino)-phenyl) acrylic acid.	38

LIST OF FIGURES (Continued)

Appendix Figure	Page
A1 I-V curve of PV cell and associated electrical diagram.	47
A2 Simplified equivalent circuit model for a photovoltaic cell.	48
A3 Illuminated I-V sweep curve.	48
A4 Getting the fill factor from the I - V sweep.	51

LIST OF ABBREVIATIONS

TPA	=	Triphenylamine
TC	=	Triphenylamine Cyanoacrylic Acid
TC1	=	2-Cyano-3-(4-(diphenylamino)phenyl)acrylic Acid
TC2	=	2-Cyano-3-(4-(phenyl(4-vinylphenyl)amino)phenyl)acrylic Acid
TC3	=	3,3'-(4,4'-(Phenylazanediyl)bis(4,1-phenylene))bis(2-cyanoacrylic Acid)
TC4	=	2-Cyano-5-(4-(phenyl(4-vinylphenyl)amino)phenyl)penta-2,4-dienoic Acid
HF	=	Hartree-Fock
DFT	=	Density Functional Theory
TD-DFT	=	Time-Dependence Density Functional Theory
B3LYP	=	Becke's three parameter hybrid functional using the LYP correlation functional
CAM-B3LYP	=	Long range corrected version of B3LYP using the Coulomb-attenuating method
PBE0	=	The Pure functional of Perdew, Burke and Ernzerhof
M06-HF	=	Meta exchange correlation function with full Hartree-Fock exchange
M06-2X	=	Meta exchange correlation function with 54% of Hartree-Fock exchange
M06	=	Meta exchange correlation function with 27% of Hartree-Fock exchange
M06-L	=	Meta exchange correlation function with no Hartree-Fock exchange
MP2	=	The second-order Møller-Plesset perturbation theory
HOMO	=	Highest Occupied Molecular Orbital
LUMO	=	Lowest Unoccupied Molecular Orbital
MO	=	Molecular Orbital

EXCITATION ENERGIES OF TRIPHENYLAMINE CYANOACRYLIC ACID FOR DYE-SENSITIZED SOLAR CELLS USING LONG-RANGE CORRECTED TIME-DEPENDENT DENSITY FUNCTIONAL THEORY

INTRODUCTION

The energy demands have led to attempt to find renewable energy which comes from natural resources such as sunlight. In 1839 Alexandre-Edmond Becquerel has discovered photovoltaic effect by his experiment. He found that the electricity increased when the light intensity increased. This was the beginning of solar cell technology. Afterward, in 1905 Albert Einstein published his paper about the photoelectric effect which claimed that light consists of photons and it explained very well the absorption of the photons regarding to the frequency of the light.

In 1954, Bell Laboratories have discovered a silicon solar cell, which was the first material to directly convert enough sunlight into electricity to run electrical devices. The efficiency of the silicon solar cells were 4%, which later increased to 15%. Therefore, the first generations of solar cells were made from silicon.

The idea of a solar cell is to convert light into electrical energy. The energy of light is photons. A solar cell is essential a P-N junction with a large surface area. The generation of electric current happens inside the depletion zone of the P-N junction. When photons are absorbed on N-Type silicon it will dislodge an electron and creating a free electron and hole. The free electron and hole has sufficient energy to jump out of the depletion zone. If a wire is connected from the cathode (N-type silicon) to the anode (P-type silicon) electrons will flow through the wire. The electron is attracted to the positive charge of the P-type material and travels through the external load (meter) creating a flow of electric current. The hole created by the dislodged electron is attracted to the negative charge of N-type material and migrates to the back electrical contact. As the electron enters the P-type silicon from the back

electrical contact it combines with the hole restoring the electrical neutrality (shown in Figure 1.)

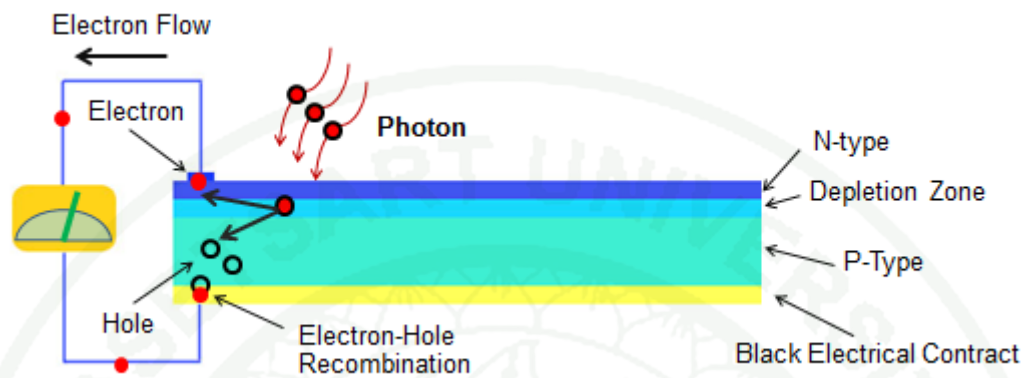


Figure 1 Generating electricity of P-N junction solar cell.

There have been many using solar-cells to convert the energy of sunlight directly into electricity. However, silicon materials for fabrication solar-cells have expensive cost. The cost of silicon processing has led many solar cell producers to turn to other semiconductor materials.

In 1991, Grätzel cells have developed solar cell based on low-cost materials. Each cell consists of a semiconducting photoanode and a metal oxide cathode immersed in an electrolyte. The new class of solar cell was called dye-sensitized solar cells (DSSCs). The benefits of the DSSCs are its simple fabrication, low cost and friendly environmentally. Although, its conversion efficiency is less than the silicon solar cells, its price/performance ratio is high enough to compete with fossil fuel electrochemical generation.

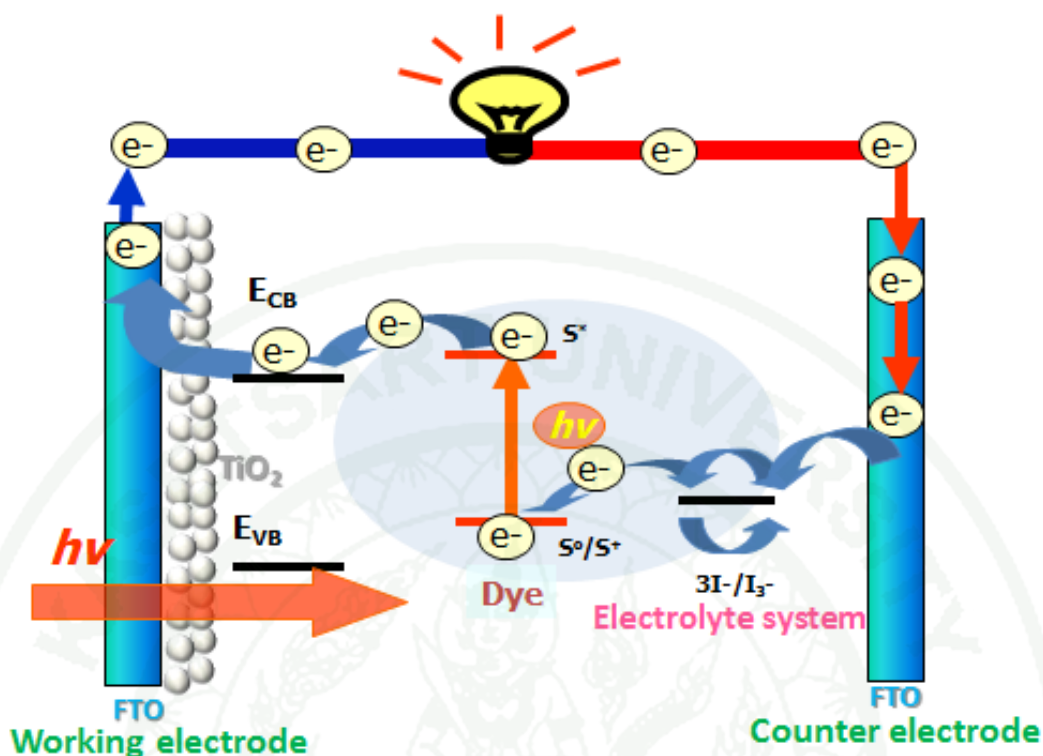


Figure 2 Components and electron flow of Dye-sensitized solar cells (DSSCs).

The working scheme of DSSCs is illustrated in Figure 2, showing a TiO_2 layer deposited in a conductive fluorine-doped tin oxide glass. The dye is placed over this semiconductor film, in contact with an electrolyte. The electron will move from ground state to excited state when the organic-dye has received sunlight, and then the electrons were injected to the conduction band of TiO_2 . The electron was collected by powering load. After flowing through the external circuit, electron will back into the cell on counter electrode then the electrolyte solution will transports the electron back to the dye molecule, while electron migration from the working electrode to the counter electrode closes the circuit. The voltage generated is equal to the difference between the Fermi level of the electron in the solid TiO_2 and the redox potential of the electrolyte.

The dye-sensitized solar cells (DSSCs) have attracted a lot of interest for their abilities to convert solar light to electricity at low cost. There have been two kinds of dyes, namely, metal-organic complexes and metal-free organic dyes. The metal-organic dye based on ruthenium sensitizer has shown very impressive solar-to-electric power conversion efficiencies (shown in Figure 3), reaching 11% at standard AM 1.5 sun light (Grätzel, 2004; Nazeeruddin *et al.*, 2005).

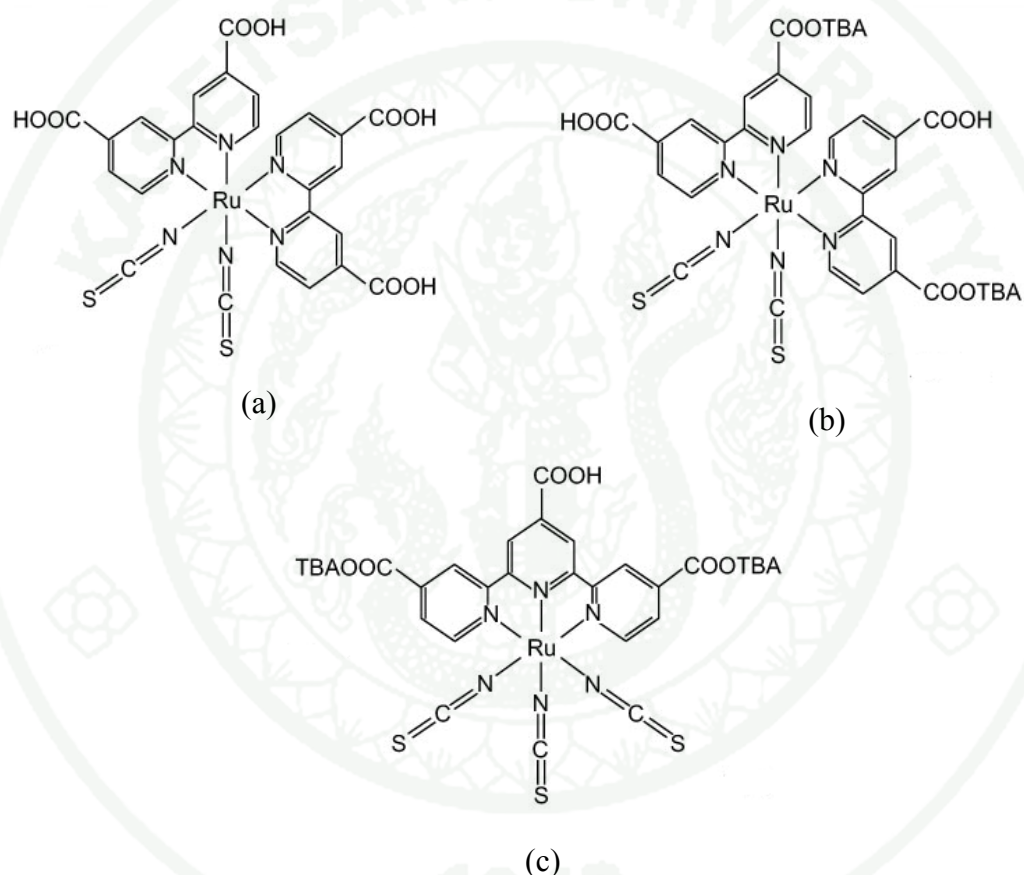


Figure 3 Structure of Ru complexes dye (a) N3, (b) N179 and (c) black dye.

Although Ru complexes are suitable as photosensitizers, the limited availability and environmental issues would limit their extensive application. In the meantime, alternative metal-free organic dyes exhibit high molar extinction coefficients and are easily modified due to short synthetic and economically, have shown the conversion efficiencies up to 8% (Ehret *et al.*, 2001; Hara *et al.*, 2002; Sayama *et al.*, 2002; Wang *et al.*, 2000). A common design of the organic sensitizer is to link the electron donor and the electron acceptor by a conjugated spacer. Then the

TiO₂ surface anchoring group, such as carboxylate, phosphonate, or sulfonate, is integrated at the acceptor end. Light irradiation on these dipolar molecules induces intramolecular charge transfer from the donor to the acceptor, with subsequent electron injection to the TiO₂ via the anchoring group. Several metal-free dyes have been reported as sensitizers in DSSCs in recent years. These include perylene, cyanine, xanthene, merocyanine, coumarin, hemicyanine, indoline, and triphenylamine dyes.

Although remarkable advance has been made in the organic dyes as sensitizers for DSSCs, but it is still needed to optimize their chemical structures for further improvement on performances. An ideal sensitizer has to fulfill the following criteria: (1) it has a sufficiently low LUMO energy level for efficient electron injection into the TiO₂ and a sufficiently High HOMO energy level for efficient regeneration of the oxidized state; (2) it absorbs solar radiation strongly, with the absorption band in the visible region extending to near-IR; (3) it possesses enough spatial separation between the positive charge density on the dye and the electrons injected (Robertson, 2006).

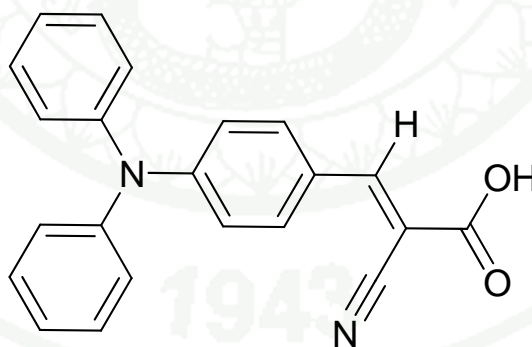


Figure 4 Molecular Structures of triphenylamine cyanoacrylic acid.

Among the metal free organic dyes, triphenylamine (TPA) and its derivatives as donor units have displayed promising properties in the development of photovoltaic devices (Sato *et al.*, 2003; Sato *et al.*, 2005; Wang *et al.*, 2005). Theoretical and experimental studies have demonstrated that TPA unit can be used as the sensitizer of DSSCs. In 2008, Xu's and coworker shown that triphenylamine moieties and a cyanoacetic acid moiety are desirable units in the design of dyes as electron donor and electron acceptor/anchoring group (shown in Figure 5), respectively. Bridge groups, as electron spacers to connect the donor and acceptor, are not only to decide light absorption regions of the DSSCs but also influence the electron injection from excited dyes to the TiO₂ surface.

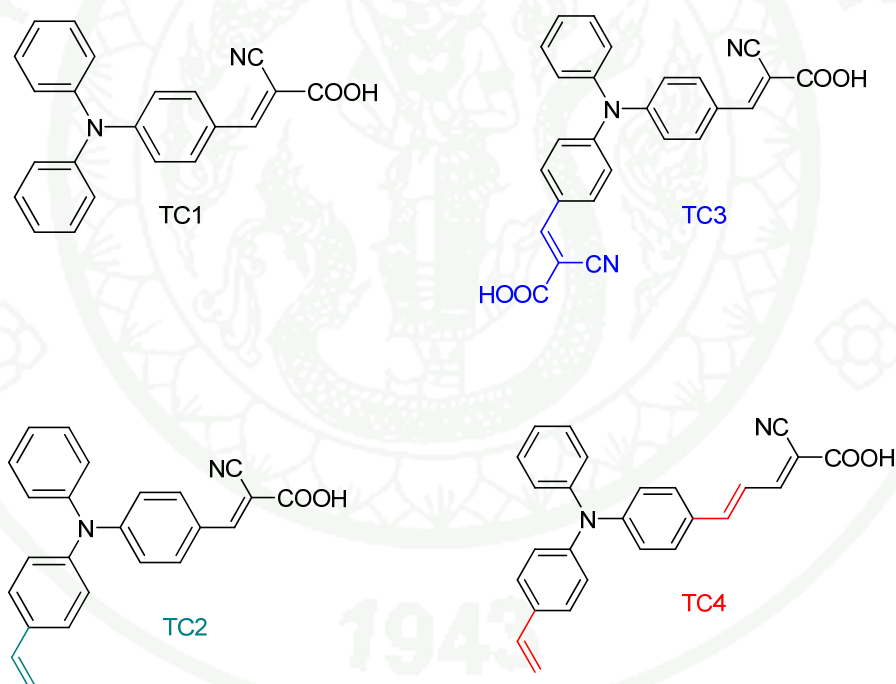


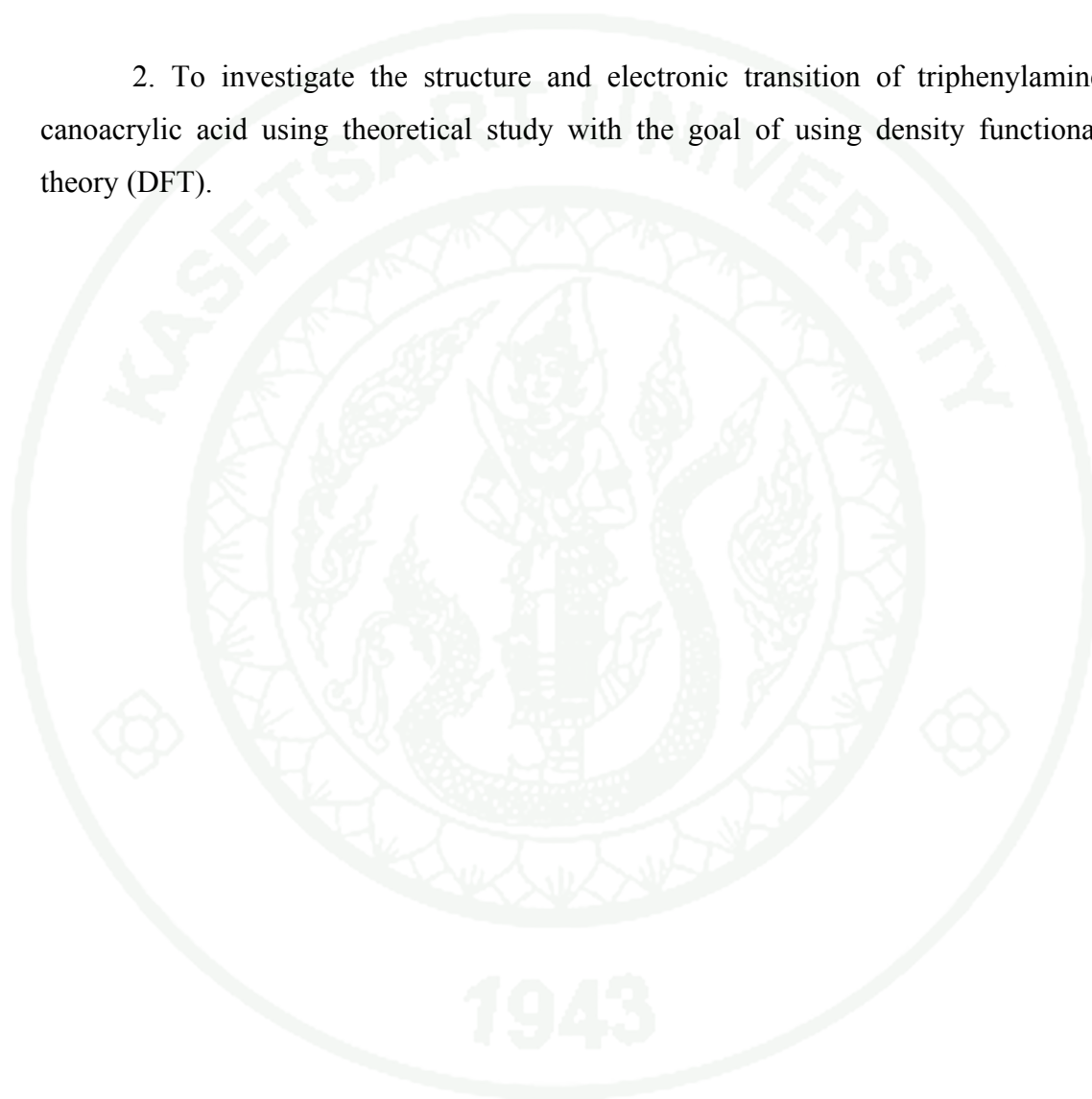
Figure 5 Molecular Structures based on triphenylamine (TPA) moieties as the donor and cyanoacetic acid moieties as the electron acceptor groups by Xu *et al.* (2008).

It is of interest to investigate the effect of electron donor and anchoring group for increase the effectively of DSSC. Accordingly, we have thus focused our investigation using theoretical study with the goal of using density functional theory (DFT) to understand and development of new sensitizer based on triphenylamine (TPA) moieties and cyanoacrylic acid moieties as the electron donor groups and electron acceptor group for solar cell applications, respectively. The quantum chemical calculations are the most appropriate alternative for understands the structure and electronic properties of molecules. Their absorption spectra in solvent phase were calculated by time-dependent density functional theory (TD-DFT) and several polarizable continuum model (PCM-TDDFT) approaches.



OBJECTIVES

1. To find suitable method for prediction absorption properties and electronic transition of triphenylamine cyanoacrylic acid and its derivatives.
2. To investigate the structure and electronic transition of triphenylamine canoacrylic acid using theoretical study with the goal of using density functional theory (DFT).



LITERATURE REVIEW

The interest in metal-free organic dyes with high extinction coefficients has grown in recent years. The design and synthesis of functional dyes have become a focus of current research in view of their potential applications as sensitizers in dye-sensitized solar cell (DSSC) technologies. The π -conjugated systems between the donor (triphenylamine moiety) and the acceptor (cyanoacetic acid moiety) were systematically extended to adjust the molecular HOMO and LUMO energy levels of the dyes. Triphenylamine-based π -conjugated have been widely used in photovoltaic cells because of their chemical and environmental stability as well as their electronic tunability.

Hagberg *et al.* (2007) tuned the HOMO and LUMO Energy Levels of Organic Chromophores for Dye Sensitized Solar Cells, which was further supported by electrochemistry and TDDFT calculations that show that these orbitals are distributed over the linker conjugation. Even though all dyes seem to fulfill the energetic criteria for DSSC the longer linker dyes showed pronounced losses. The longer linker conjugation gives increased spectral response but increases recombination of electrons to the triiodide. Solar cells based on 3-(5-(4-(Diphenylamino)styryl)thiophen-2-yl)-2-cyanoacrylic Acid (L2) yielded the highest efficiency. The L2 chromophore is thus showing the optimal properties in this study considering the energy levels and other parallel effects, arising when varying the linker conjugation.

In 2008, this group has developed a series of unsymmetrical organic sensitizers, which demonstrate the effect of substituted donor groups on controlling optical and photovoltaic properties. The unsymmetrical organic sensitizers anchored onto TiO_2 and were tested in dye-sensitized solar cell with a volatile electrolyte. The monochromatic incident photon-to-current conversion efficiency of these sensitizers is above 80%, and 3-(5-bis(4,4'-dimethoxy-diphenylamino)styryl)thiophen-2-yl)-2-cyanoacrylic acid (D11) sensitized solar cells exhibit the highest overall conversion efficiency of 7.20% under standard AM 1.5 sun light. Detailed investigations of these sensitizers reveal that the long electron lifetime is responsible for differences in

observed open-circuit potential of the cell. Density functional theory/time-dependent density functional theory calculations have been employed to gain insight into the electronic structure and excited states of the investigated species.

Li *et al.* (2008) designed synthesized, and characterized a series of new organic D- π -A dyes based on di(*para*-tolyl)phenylamine moiety as an electron donor, a cyanoacetic acid moiety as an electron acceptor/anchoring group, and different types of conducting thiophene units as electron spacers to bridge the donor and acceptor. These dyes were developed as sensitizers for the application in dye-sensitized TiO₂ nanocrystalline solar cells (DSSCs). The DSSCs basedd on the dyes gave good performance in terms of incident photon-to-current conversion efficiency (IPCE) in the range of 400-700 nm. A solar-energy-to-electricity conversion efficiency (η) of 7.00% was obtained with the DSSC basedd on 5-[2-[p-(di-*p*-tolylamino)]styryl]thiophene-yl]thiophene-2-cyanoacrylic acid and the density functional theory (DFT) calculation suggests that the electron-transfer distribution moves from the donor unit to the acceptor under light irradiation

Xu *et al.* (2008) designed a series of new conjugated metal free organic dyes comprising triphenylamine (TPA) moieties as the electron donor and cyanoacetic acid moieties as the electron acceptor/anchoring groups and developed for the use in dye-sensitized solar cells (DSSCs). They have used quantum chemical calculations to gain insight into structural, electronic, and optical properties of the as-synthesized sensitizers. They found that the photovoltaic performance of the DSSCs with the as-synthesized dyes can be improved by enhancing the electron-donor ability and extending the π -conjugated bridge of the dyes. In particular, the DSSCs basedd on 2-cyano-5-(4-(phenyl(4-vinylphenyl)amino)phenyl) penta-2,4-dienoic acid dye showed electricity conversion efficiency of 4.82% under AM 1.5 irradiation. This result reveals that efficient electron injection from the excited sensitizer to the conduction band of titania film occurs.

Liu *et al.* (2008) reported design and syntheses of a series of simple organic dyes that contain common triphenylamine (TPA) as donor and cyanoacrylic acid or rhodanine-3-acetic acid as electron acceptor (anchoring groups). These two moieties are bridged by thiophene and its derivatives, such as 3,4-ethylene dioxythiophene (EDOT) or 3,4-bis[2-(2-methoxy-ethoxy)ethoxy]thiophene (BMEET) to form organic dyes. They found the EDOT can increase the spectral response and perhaps renders a better degree of charge separation, also exhibits a conversion efficiency η as high as

7.3%.

Thomas *et al.* (2008) have synthesized and studied a new class of dyes featuring oligothiophene conjugation, diarylamines as electron donors at the 2- and 3-sites, and 2-cyanoacrylic acids as electron acceptors. They have found incorporation of a hydrophobic arylamine-containing segment at the 3-position of the thiophene spacer was demonstrated to be beneficial for retarding the electron transfer from TiO_2 to the oxidized dye or electrolyte and to enhance the charge transfer efficiency in the excited state. The devices in this study appear to have efficiencies comparable to those of the oligothiophene-based sensitizer. It thus is likely that incorporation of appropriate alkyl chains in the thiophene rings will further improve the performance of the cells.

Yang *et al.* (2008) synthesized and investigated the triphenylamine (TPA)-based multiple electron acceptor dyes (TPAR1, TPAR2, and TPAR3) as well as their applications in dye-sensitized solar cells (DSSCs). The TPA group and the rhodanine-3-acetic acid play the role of the basic electron donor unit and the electron acceptor, respectively. They found that introduction of two rhodanine-3-acetic acid groups into the TPA unit (TPAR2) exhibited better photovoltaic performance due to the increase with a red shift and broadening of the absorption spectrum. The TPAR2-based gel

DSSC had an open circuit voltage and short circuit current density of about 541 and 10.7 mA cm^{-2} , respectively

Song *et al.* (2009) designed and synthesized the four metal-free organic dyes (Dye-1, Dye-2, Dye-3, and Dye-4) comprising a triphenylamine moiety as the electron donor, a cyanoacrylic acid or carboxylic acid moiety as the electron acceptor and anchoring groups, and phenylethyne as the bridge for use in dye-sensitized solar cells (DSSCs). Their absorption spectra and electrochemical and photovoltaic properties were calculated using density functional theory at the B3LYP/6-31G level and all of these dye were also performed as sensitizers for the DSSC test. The cyanoacrylic acid Dye-4 showed an overall conversion efficiency of 3.61% under AM 1.5 irradiation (100 mW/cm^2), which reached 79% with respect to that of an N719-based device fabricated under similar conditions.

Srinivas *et al.* (2009) studied the binding modes of anchoring groups on the nanocrystalline TiO_2 (101) surface and on the efficiency of dye-sensitized solar cells (DSSCs). The sensitizers have a monocarboxylic acid group have shown marginally higher IPCE and efficiency than M3 and M4 having dicarboxylic acid groups. The absorption and binding energies to the TiO_2 surface of these dyes have been investigated using computational techniques (periodic DFT). The studies show that the cyanoacrylic acid anchoring group has a stronger binding to the TiO_2 surface compared to the malonic acid anchoring group.

Teng *et al.* (2010) have designed and synthesized metal-free organic dyes bridged by anthracene-containing π -conjugations as new chromophores for the application of dye-sensitized solar cells (DSSCs). They investigated on the relationship between the dye structures, photophysical properties, electrochemical properties, and performances of DSSCs. With the introduction of the anthracene moiety, together with a triple bond for the fine-tuning of molecular planar configurations and to broaden absorption spectra, the short-circuit photocurrent

densities (I_{sc}) and open-circuit photovoltages (V_{oc}) of DSSCs were improved to a large extent. On the basis of optimized molecular structures and DSSC test conditions the dye 3-(4-(10-(4-(Bis(4-methoxyphenyl)amino)phenyl)anthracen-9-yl)ethynyl)phenyl)-2-cyanoacrylic Acid (TC501) shows a prominent solar energy conversion efficiency (η) up to 7.03% under simulated AM 1.5 irradiation.

Pastore *et al.* (2010) calculated the ground state oxidation potential (GSOP) and excited state oxidation potential (ESOP) of four triphenylamine-based dyes for dye-sensitized solar cell (DSSC) applications, with increasing degree of charge transfer using ab initio methods. The performance of DFT in predicting GSOP is evaluated by employing various exchange-correlation (x-c) functionals, with different amounts of Hartree–Fock exchange and different combinations of correlation functionals. The choice of the correlation part of the x-c functional was crucial in getting accurate GSOPs. They used hybrid functionals with a large amount (50%) of nonlocal Hartree–Fock exchange, for mandatory to avoid the formation of artificial minima in correspondence of twisted geometries with a high degree of charge transfer. Their results show that a proper DFT/TDDFT approach can provide a reliable description, within 0.2–0.3 eV, of both GSOP and ESOP compared to experimental values. They gave the way, along with the absorption spectra simulation, to the efficient computational screening of new dyes for DSSC devices.

Zhang *et al.* (2010) synthesized a conjugated polymer containing an electron donating backbone (triphenylamine) and an electron accepting side chain (cyanoacetic acid) with conjugated thiophene units as the linkers. These materials were used as the dye sensitizer in dye-sensitized solar cells (DSSCs). The results show that power conversion efficiency of 3.39% under AM 1.5 G illumination, which represents the highest efficiency for polymer dye-sensitized DSSCs reported so far. The results show the good promise of conjugated polymers as sensitizers for DSSC applications.



MATERIALS AND METHODS

Synthesis and Characterization

1. Materials

- 4-(Diphenylamino)benzaldehyde ($C_{19}H_{15}NO$)
- Cyanoacetic acid ($NCCH_2COOH$)
- Glacial acetic acid (CH_3CO_2H)
- Ammonium acetate ($CH_3CO_2NH_4$)
- Distilled water (H_2O)

2. Instruments

1H -NMR analyses was carried out using a VARIAN ^{UNITY} INOVA spectrometer which operated at 400.00 MHz for 1H in deuterated chloroform ($CDCl_3$) with tetramethylsilane (TMS) as an internal reference. UV analysis was done with Perkin Elmer Lambda 35 UV-Vis spectrophotometer, using a quartz cell with 1 cm path length.

3. Synthesis

The solid state structure of 2-cyano-3-(4-(diphenylamino)-phenyl) acrylic acid (TC1) have been investigated (Figure 6).

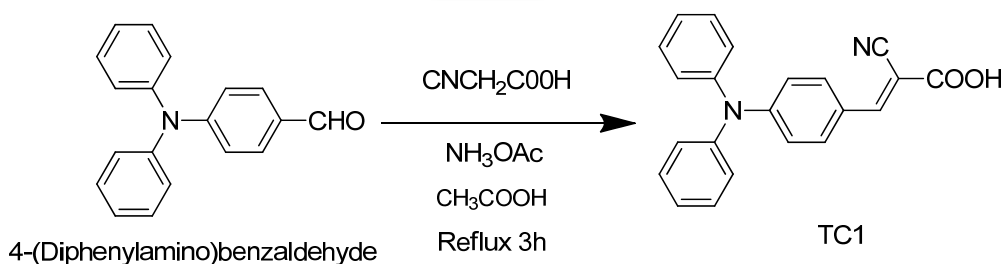


Figure 6 Synthesis rout of 2-cyano-3-(4-(diphenylamino)-phenyl) acrylic acid (TC1).

4-(Diphenylamino)benzaldehyde (273 mg, 1 mmol) and cyanoacetic acid (128 mg, 1.5 mmol) were added to 15 mL of glacial acetic acid and refluxed for 3 hour in the presence of 150 mg of ammonium acetate. After cooling to room temperature, the mixture was poured into ice water. The precipitate was filtered, washed by distilled water, dried under vacuum, resulting in yellow powder of TC1.

$^1\text{H-NMR}$ (CDCl_3 , δ ppm): 8.1 (1H, s, -CH), 7.85 (2H, d, -Ar-H), 7.35 (4H, t, -Ar-H), 6.95 (2H, d, -Ar-H), 7.16-7.24 (6H, m, -Ar-H)

Quantum Chemical Calculations

1. Ground state calculations

The starting geometries of triphenylamine cyanoacrylic acid and its derivatives (in Figure 5) were constructed by GaussView 3.0 program. The triphenylamine cyanoacrylic acid and its derivatives structures were fully optimized using quantum chemical calculations with *ab initio* and density functional theory (DFT) methods.

First of all, the starting structure of triphenylamine (TPA) was fully optimized by using *ab initio* method with Hartree-Fock (HF), 2nd order Moller-Plesset Perturbation Theory (MP2) methods and DFT method with B3LYP hybrid functional together at 6-31G(d) level of basis set. The geometrical parameters that obtained from optimization such as bond length, bond angle, and bond torsion angle are compared with X-ray crystallography data (Naumov *et al.*, 2005) with the mean relative errors of bond length that is then defined as

$$\text{The mean relative errors} = \sum_{i=1}^n \frac{|X_{Cal} - X_{Exp}|}{|X_{Exp}|} \bigg/ n$$

The starting structure of 2-cyano-3-(4-(diphenylamino)-phenyl) acrylic acid (TC1) was also fully optimized using server DFT methods such as B3LYP, M06, M06-HF, M06-L, M06-2X together with 6-31G(d) level of basis set.

Furthermore, the triphenylamine cyanoacrylic acid derivatives (TC1, TC2, TC3 and TC4) were fully optimized using M06-HF method together with 6-31G(d,p) level of basis set. The geometries of these compound in their neutral, cationic, and anionic states were also optimized at M06-HF/6-31G(d,p) level in vacuo without symmetry constraints. The neutral, cationic, and anionic forms of these compounds were used to compute the ionization potential (IP) and electron affinity (EA).

2. Excited state calculations

The excitation energies of TC1 were performed based on the ground state geometries using time-dependent density functional theory (TD-DFT) with B3LYP at 6-311G(d,p) level of basis set in gas phase to predict the absorption properties and compared with experimental data.

The optimized structure of TC1 obtained from M06-HF method was also calculated the excitation energies using several TD-DFT functional, PBE0, LC-B3LYP, LC-wPBE, CAM-B3LYP together with 6-311G(d,p) level of theory including conductor polarizable continuum model (PCM) solvation. Moreover, the excitation energies of all triphenylamine cyanoacrylic acid (structures of TC1, TC2, TC3 and TC4 shown in Figure 5) derivatives were calculated using CAM-B3LYP method at 6-311G(d,p) in solvent phase. We study the low-lying excited states of all molecules in various solutions using long-range corrected TDDFT.

The solvation effect on transition energies has been evaluated by means of the PCM approach. The dielectric constant of methanol ($\epsilon = 32.613$) was used in accordance with the measurement of the UV-vis spectra. For absorption, geometry optimization of the ground state (S_0) was performed with equilibrium approach and the PCM-TD-DFT calculations were performed with non-equilibrium scheme. Bulk solvent effect on the excited state was calculated with the linear-response (LR) and state-specific (SS) solvation approach. The results from calculations were compared with the experimental data from Xu's and coworker. All of calculations were carried out by the GAUSSIAN09 program package.

RESULTS AND DISCUSSION

1 Method validation based on ground state optimization by triphenylamine structure

The optimized geometrical parameter using *ab initio* method with HF, MP2 methods and DFT approach with B3LYP hybrid functional together at 6-31G(d) level of basis set were compared with X-ray crystallographic data that reported by Naumov *et al.*, 2005 are shown in Table 1. This table is showing bond lengths, bond angles, torsion angles and means relative error of triphenylamine structure which atom numbering are shown in Figure 7.

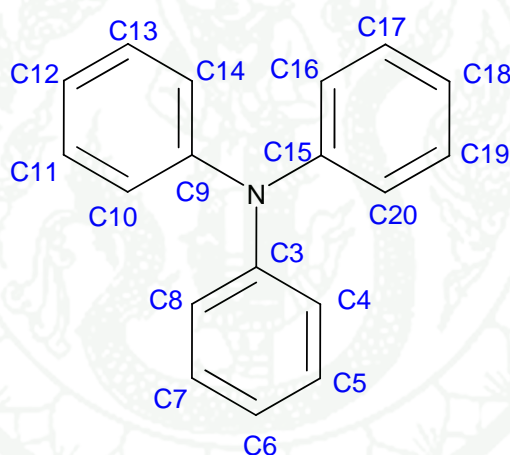


Figure 7 Conformation of triphenylamine and atom numbering scheme.

The bond length comparison between theoretical data and X-ray data indicating that HF method underestimated bond length. Conversely, the bond length comparison from DFT approach with B3LYP and MP2 methods are near close to X-ray crystallographic data which are presented in Figure 8.

For the comparison of bond angle and torsion angle, each method correspond to X-ray crystallographic data, except bond angle of N-C3-C8 and N-C3-C4 are different with X-ray data (shown in Figure 9). From the theoretical results indicating that the structure of triphenylamine is not coplanar structure.

Table 1 Structural parameters of triphenylamine obtained from full optimization using HF, B3LYP and MP2 methods at 6-31G(d) level of basis set (Bond length in angstrom, Angle in degrees). The mean relative error values are also listed.

Parameter	HF	B3LYP	MP2	X-ray ^a
<i>Bond length</i>				
N-C3	1.416	1.422	1.414	1.418
C3-C4	1.391	1.405	1.404	1.404
C4-C5	1.384	1.393	1.394	1.396
C5-C6	1.385	1.397	1.397	1.397
C6-C7	1.385	1.396	1.397	1.397
C7-C8	1.384	1.394	1.394	1.396
C8-C3	1.391	1.404	1.404	1.404
C4-H	1.074	1.085	1.087	
C5-H	1.076	1.087	1.088	
C6-H	1.075	1.086	1.087	
<i>Bond angle</i>				
∠(N-C3-C4)	120.5	120.5	120.3	123.4
∠(N-C3-C8)	120.5	120.5	120.3	117.5
∠(C-N-C)	120.0	120.0	120.0	119.9
∠(C4-C3-C8)	119.0	118.9	119.5	119.1
∠(C3-C4-C5)	120.4	120.3	120.0	120.3
∠(C4-C5-C6)	120.6	120.6	120.6	120.6
∠(C5-C6-C7)	119.2	119.2	119.3	119.2
∠(C6-C7-C8)	120.6	120.6	120.6	120.7
∠(C7-C8-C3)	120.3	120.3	120.0	120.2
<i>Torsion angle</i>				
τ(C4-C3-N-C9)	46.1	42.4	40.1	45.2
τ(C3-N-C9-C14)	46.1	41.0	40.1	39.2
<i>Relative Error</i>	0.0078	0.0011	0.0008	N/A

Sources: ^aXu *et al.* (2008)

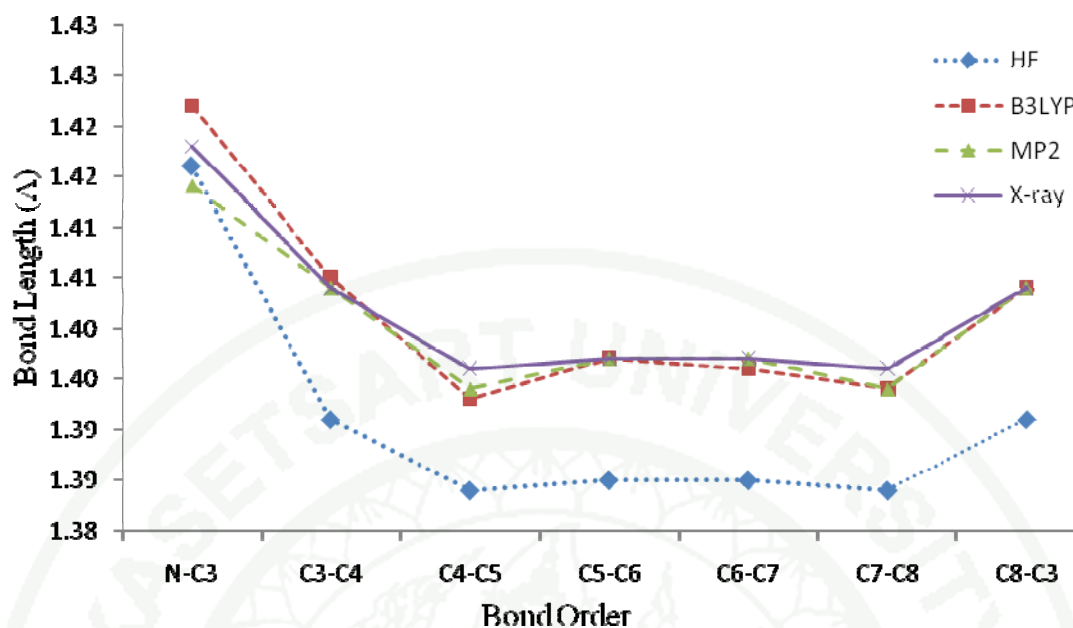


Figure 8 Bond lengths of triphenylamine obtained from various methods are compared with X-ray^a data.

Sources: ^aXu *et al.* (2008)

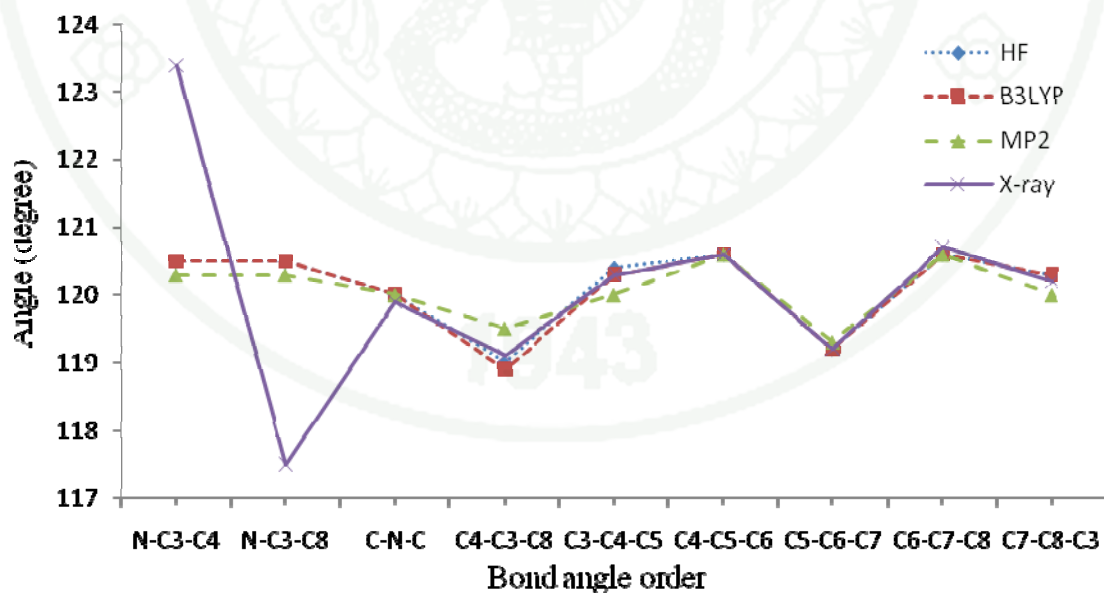


Figure 9 Bond angle of triphenylamine obtained from various methods are compared with X-ray^a data.

Sources: ^aXu *et al.* (2008)

To simplify the comparison of triphenylamine, its bond length and bond angle are also reported in an average value. The mean relative errors (0.0078, 0.0011 and 0.0008) obtained from HF/6-31G(d), B3LYP/6-31G(d) and MP2/6-31G(d) methods, respectively. To save time consuming cost, the DFT approach was therefore chosen for optimize the starting geometries structure of triphenylamine cyanoacrylic acid derivatives.

2 Method validations of DFT calculated on the electronic transition by TC1 structure

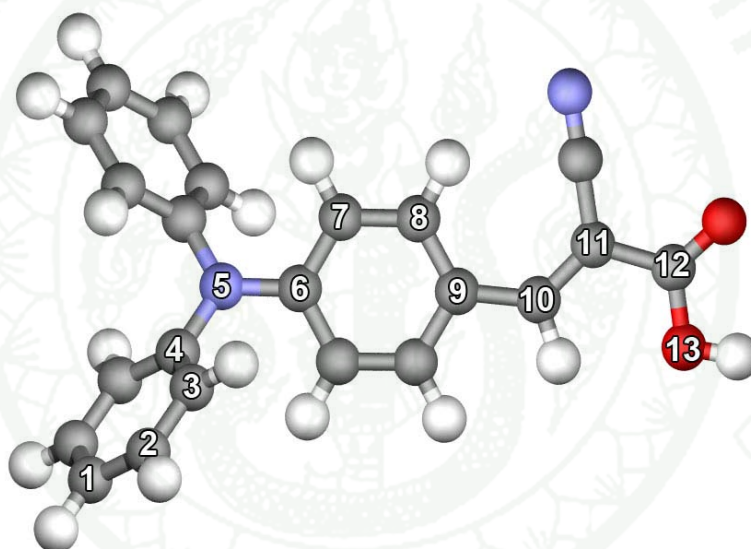


Figure 10 Equilibrium structure of 2-cyano-3-(4-(diphenylamino)phenyl) acrylic acid (TC1) and atom numbering.

The starting geometries structure of 2-cyano-3-(4-(diphenylamino)phenyl) acrylic acid (TC1) was optimized in several DFT methods, B3LYP, M06, M06-HF, M06-L and M06-2X together with 6-31G(d,p) level of basis sets. The equilibrium structure is shown in Figure 10. Afterwards, the excitation energies and oscillator strengths for the transition from ground state (S_0) to first (S_1), second (S_2), and third singlet excited state (S_3) of the molecule were calculated using TD-DFT functional in gas phase with B3LYP at 6-31G(d,p) level of theory.

The structural parameters from several DFT methods are shown in Table 2. The results show that the structural parameters of each method is not statistically significant different. Therefore, we focus on the electronic transition and absorption properties from TD-DFT calculation. The comparisons of the predicted values to the absorption band of this molecule in methanol (Xu *et al.* 2008) were presented in Table 3.

Table 2 Structural parameters of 2-Cyano-3-(4-(diphenylamino)phenyl)acrylic acid obtained from full optimization by B3LYP and M06 functional at 6-31G(d) level of basis set (Bond length in angstrom, Angle in degrees).

Parameter	B3LYP	M06L	M06	M062X	M06HF
<i>Bond length</i>					
C1-C2	1.397	1.393	1.392	1.393	1.393
C2-C3	1.394	1.390	1.389	1.391	1.391
C3-C4	1.403	1.399	1.396	1.398	1.397
C4-N5	1.430	1.422	1.423	1.423	1.422
N5-C6	1.399	1.395	1.393	1.396	1.393
C6-C7	1.414	1.411	1.408	1.408	1.407
C7-C8	1.383	1.378	1.378	1.381	1.382
C8-C9	1.415	1.414	1.410	1.409	1.405
C9-C10	1.444	1.435	1.439	1.450	1.462
C10-C11	1.369	1.370	1.363	1.357	1.347
C11-C12	1.484	1.475	1.476	1.486	1.493
C12-O13	1.361	1.359	1.351	1.350	1.344
<i>Torsion angle</i>					
τ (C8-C9-C10-C11)	0.31	0.86	0.86	0.98	0.46
τ (C9-C10-C11-C12)	179.80	179.43	179.94	179.62	179.83
τ (C10-C11-C12-C13)	0.03	0.43	0.47	0.38	0.99

Table 3 Vertical excitation (E_{ex}) of TC1 obtained from TD-B3LYP/6-31G(d,p) method in gas phase based on ground state geometries, and the experimental absorption wavelength in the methanol solvent.

Ground state geometry optimization	State	Transition ^a	E_{ex}		f^b
			nm	eV	
B3LYP /6-31G(d)	$S_0 \rightarrow S_1$	H \rightarrow L (82%)	415	2.98	0.77
	$S_0 \rightarrow S_2$	H \rightarrow L+1 (80%)	313	2.96	0.02
	$S_0 \rightarrow S_3$	H \rightarrow L+2 (82%)	297	4.17	0.13
M06/6-31G(d)	$S_0 \rightarrow S_1$	H \rightarrow L (82%)	412	3.01	0.77
	$S_0 \rightarrow S_2$	H \rightarrow L+1 (84%)	313	3.97	0.03
	$S_0 \rightarrow S_3$	H \rightarrow L+2 (85%)	296	4.19	0.12
M06-HF/6-31G(d)	$S_0 \rightarrow S_1$	H \rightarrow L (84%)	410	3.02	0.71
	$S_0 \rightarrow S_2$	H \rightarrow L+1 (87%)	315	3.94	0.02
	$S_0 \rightarrow S_3$	H \rightarrow L+2 (89%)	297	4.18	0.13
M06-L/6-31G(d)	$S_0 \rightarrow S_1$	H \rightarrow L (82%)	427	2.90	0.74
	$S_0 \rightarrow S_2$	H \rightarrow L+1 (82%)	315	3.94	0.02
	$S_0 \rightarrow S_3$	H \rightarrow L+2 (87%)	300	4.14	0.12
M06-2X/6-31G(d)	$S_0 \rightarrow S_1$	H \rightarrow L (83%)	418	2.97	0.71
	$S_0 \rightarrow S_2$	H \rightarrow L+1 (85%)	315	3.94	0.02
	$S_0 \rightarrow S_3$	H \rightarrow L+2 (88%)	298	4.16	0.13
Absorption data ^c			400	3.10	

^a H = HOMO, L = LUMO, H-1 = next highest occupied molecular orbital, or HOMO-1, and L1 = LUMO+1. ^b Oscillator strength. ^c Xu *et al.* (2008)

The result from TD-B3LYP calculations on all ground state geometries are used to predict the oscillator strength and maximum absorption wavelength. It is found that the $S_0 \rightarrow S_1$ transition corresponding to the excitation from the HOMO to the LUMO is dominant. The absorption wavelengths of the transition obtained from the ground state geometries optimized using B3LYP, M06, M06-HF, M06-L and M06-2X are 415, 412, and 410, 427 and 418 nm, respectively. These results are in well agreement with experimental absorption data. However, the maxima absorption wavelength from M06-HF method is closer to experimental data of 400 nm than that of another method.

The results from Table 3, indicating that the results from ground state geometries of TC1 molecule using M06-HF together with 6-31G(d) level of basis set is in well agreement than another DFT methods. For the accuracy of calculation, the M06-HF/6-31G(d) method is therefore chosen for the ground state geometry optimization.

Therefore, the excitation energies of TC1 were also calculated using several TD-DFT functional, PBE0, LC-B3LYP, LC-wPBE, CAM-B3LYP at 6-311G(d,p) level of theory including conductor polarizable continuum model (PCM) solvation basedd on the optimized structures obtained from M06-HF/6-31G(d) method. The computed vertical excitation energies for singlet excited states, together with the oscillator strength and maximum absorbance calculated using different functional, compared to experimental results are shown in Table 4. The results from Table 4 are indicating that the LR-PCM-TD-PBE0 overestimated maximum absorbance wavelength at 429 nm. On the other hand, the other method underestimated maximum absorbance, due to LC-BLYP, LC-wPBE and CAM-B3LYP were added long rang correction in functions. From the observation, the maximum absorbance using LR-PCM-TD-CAM-B3LYP/6-311G(d,p) methods at 375 nm are in better agreement with the experimental results at 400 nm than the other LR-PCM-TD-DFT functional, PBE0 (429 eV), LC-B3LYP (335 eV) and LC-wPBE (340 eV).

We conclude in this part that PCM-TD-CAM-B3LYP/6-311G(d,p) is reliable methods for prediction absorption properties of 2-cyano-3-(4(diphenylamino)phenyl) acrylic acid (TC1) and its derivative.

Table 4 Vertical excitation (E_{ex} (eV)) of TC1 molecule obtained from PCM-TD-DFT methods in methanol at 6-311G(d,p) basis set based on ground state geometries.

Methods	States	E_{ex} (eV)	λ_{max} (nm)	f	Transition
PBE0	$S_0 \rightarrow S_1$	2.89	429	0.839	H \rightarrow L (99%)
	$S_0 \rightarrow S_2$	3.98	312	0.023	H \rightarrow L+1 (90%)
	$S_0 \rightarrow S_3$	4.28	290	0.175	H \rightarrow L+2 (94%)
	$S_0 \rightarrow S_4$	4.36	284	0.155	H-1 \rightarrow L (92%)
LC-BLYP	$S_0 \rightarrow S_1$	3.71	335	1.104	H \rightarrow L (80%)
	$S_0 \rightarrow S_2$	4.73	262	0.022	H \rightarrow L+1 (62%)
	$S_0 \rightarrow S_3$	5.06	245	0.241	H \rightarrow L+2 (76%)
	$S_0 \rightarrow S_4$	5.17	240	0.018	H \rightarrow L+4 (22%)
LC-wPBE	$S_0 \rightarrow S_1$	3.65	340	1.093	H \rightarrow L (81%)
	$S_0 \rightarrow S_2$	4.66	266	0.022	H \rightarrow L+1 (64%)
	$S_0 \rightarrow S_3$	4.99	249	0.247	H \rightarrow L+2 (76%)
	$S_0 \rightarrow S_4$	5.11	243	0.018	H \rightarrow L+4 (25%)
CAM-B3LYP	$S_0 \rightarrow S_1$	3.31	375	1.006	H \rightarrow L (92%)
	$S_0 \rightarrow S_2$	4.34	286	0.025	H \rightarrow L+1 (78%)
	$S_0 \rightarrow S_3$	4.66	266	0.214	H \rightarrow L+2 (86%)
	$S_0 \rightarrow S_4$	4.80	258	0.025	H-5 \rightarrow L(33%)

^aExperimental; Absorption energy (λ_{max})= 400 nm

3 Electronic transition using TD-CAM-B3LYP with various PCM methods

The structures of triphenylamine cyanoacrylic acid derivatives (TC1, TC2, TC3 and TC4) were optimized using M06-HF/6-31G(d) level of theory. The structural parameters of all molecules in bond length and bond angle are not different, except C1-N-C7-C8 and C2-C1-N-C7 torsion angle.

Table 5 Structural parameters of TC1, TC2, TC3 and TC4 obtained from full optimization by M06-HF functional at 6-31G(d,p) level of basis set (Bond length in angstrom, Angle in degrees).

Parameter	TC1	TC2	TC3	TC4
<i>Bond length</i>				
C1-C2	1.393	1.398	1.405	1.398
C2-C3	1.391	1.389	1.384	1.389
C3-C4	1.397	1.396	1.403	1.397
C4-N5	1.422	1.421	1.403	1.418
N5-C6	1.393	1.394	1.404	1.401
C6-C7	1.407	1.408	1.403	1.406
C7-C8	1.382	1.382	1.384	1.383
C8-C9	1.405	1.405	1.404	1.402
C9-C10	1.462	1.462	1.466	1.469
C10-C11	1.347	1.348	1.346	1.347
C11-C12	1.493	1.493	1.495	1.492
C12-O13	1.343	1.344	1.342	1.334
<i>Torsion angle</i>				
τ (C9-C10-C11-C12)	179.84	179.74	179.43	179.93
τ (C10-C11-C12-C13)	0.94	0.40	0.43	-

The solvation effect on transition energies has been evaluated by means of the PCM approach. Bulk solvent effect on the excited state was calculated with the linear-response (LR) and state-specific (SS) solvation approach. The results of the low-lying dipole-allowed excited states obtained by different PCM methods of calculation, TD-CAM-B3LYP functional at 6-311G(d,p) basis set are presented in Table 4 for the TC1 molecule.

Table 6 Vertical excitation of TC1 molecule obtained from TD-CAM-B3LYP/6-311G(d,p) that was calculated in gas phase and various PCM methods.

Methods	States	E_{ex} (eV)	λ_{max} (nm)	f	Transition
Gas	$S_0 \rightarrow S_1$	3.51	354	0.908	H \rightarrow L (92%)
	$S_0 \rightarrow S_2$	4.33	286	0.024	H \rightarrow L+1 (81%)
	$S_0 \rightarrow S_3$	4.64	267	0.172	H \rightarrow L+2 (89%)
	$S_0 \rightarrow S_4$	4.82	257	0.014	H \rightarrow L+5 (20%)
LR-PCM	$S_0 \rightarrow S_1$	3.31	375	1.006	H \rightarrow L (92%)
	$S_0 \rightarrow S_2$	4.34	286	0.025	H \rightarrow L+1 (78%)
	$S_0 \rightarrow S_3$	4.66	266	0.214	H \rightarrow L+2 (86%)
	$S_0 \rightarrow S_4$	4.80	258	0.025	H-5 \rightarrow L (33%)
SS-PCM	$S_0 \rightarrow S_1$	3.15	393	1.197	H \rightarrow L (91%)
	$S_0 \rightarrow S_2$	4.32	287	0.047	H \rightarrow L+1 (81%)
	$S_0 \rightarrow S_3$	4.60	270	0.317	H \rightarrow L+2 (86%)
	$S_0 \rightarrow S_4$	4.77	260	0.075	H-5 \rightarrow L (31%)
Experiment		3.10	400		

The vertical excitation energies in solution, methanol, are also evaluated within the PCM approach. In the PCM, the equilibrium linear response (LR-PCM-TD-DFT) and state-specific (SS-PCM-TD-DFT) approaches were performed and also compared with the vertical excitation energies in gas phase. The maximum absorbance in gas phase was increased from 354 nm to 375 and 393 nm for calculating by LR-PCM and SS-PCM approaches, respectively. The result shown that the vertical excitation energies were improved when we applied the state specific (SS) in PCM method and are close with experimental data (400 nm).

From our results indicate that state specific version of PCM-TD-DFT provides more reliable results than its LR counterpart. The maximum absorbance was red-shift from 375 nm to 393 nm in state specific model. Furthermore, the SS model was also applied in another PCM-TD-DFT functional, but the results that provided are not corresponding with experimental data, the PPE0 method is still overestimate maximum absorbance, LC-BLYP and LC-wPBE are still underestimate maximum absorbance. The results from Table 7 are still indicating that CAM-B3LYP is suitable method for prediction maximum absorbance wavelength when we applied SS model in PCM method.

The molecular orbitals of TC1 from the electronic transition results were examined with SS-PCM-TD-CAM-B3LYP/6-311G(d,p) based on ground state geometries optimization at M06-HF/6-31G(d). The assignments of all peaks are almost identical to those of the TD-CAM-B3LYP calculations. The first peak was assigned to the transition from HOMO to LUMO and the second peak, was ascribed to the linear combination of HOMO→LUMO+2 components. All of these states are assigned to the $\pi \rightarrow \pi^*$ transition. The relevant MOs for these transitions are shown in Figure 11.

The observation of the frontier orbitals of the dyes shows that the HOMO of TC1 is delocalized over the entire molecule. Simultaneously, the LUMO of both are still delocalized over the entire molecule. Nevertheless, the LUMO of both are mainly delocalized over the cyanoacrylic group. The $S_0 \rightarrow S_1$ transition has the highest oscillator strength thus the most probable transition, corresponding to excitation from HOMO to LUMO. It can be identified that the absorption band of this compound is attributed to $\pi \rightarrow \pi^*$ transition.

Table 7 Vertical excitation of TC1 molecule obtained from several SS-PCM-TD-DFT methods in methanol at 6-311G(d,p) basis set based on ground state geometries and experiment data^a.

Methods	State	Excitation			Transition
		E_{ex} (eV)	λ_{max} (nm)	f	
PBE0	$S_0 \rightarrow S_1$	2.74	452	1.034	H \rightarrow L (99%)
	$S_0 \rightarrow S_2$	3.96	313	0.043	H \rightarrow L+1 (92%)
	$S_0 \rightarrow S_3$	4.22	294	0.271	H \rightarrow L+2 (95%)
	$S_0 \rightarrow S_4$	4.31	288	0.207	H-1 \rightarrow L (93%)
LC-BLYP	$S_0 \rightarrow S_1$	3.55	349	1.290	H \rightarrow L (79%)
	$S_0 \rightarrow S_2$	4.71	263	0.042	H \rightarrow L+1 (65%)
	$S_0 \rightarrow S_3$	4.99	248	0.356	H \rightarrow L+2 (76%)
	$S_0 \rightarrow S_4$	5.15	241	0.047	H \rightarrow L+4 (17%)
LC-wPBE	$S_0 \rightarrow S_1$	3.49	355	1.280	H \rightarrow L (81%)
	$S_0 \rightarrow S_2$	4.64	267	0.041	H \rightarrow L+1 (66%)
	$S_0 \rightarrow S_3$	4.92	252	0.362	H \rightarrow L+2 (76%)
	$S_0 \rightarrow S_4$	5.08	244	0.049	H \rightarrow L+4 (19%)
CAM-B3LYP	$S_0 \rightarrow S_1$	3.15	393	1.197	H \rightarrow L (91%)
	$S_0 \rightarrow S_2$	4.32	287	0.047	H \rightarrow L+1 (81%)
	$S_0 \rightarrow S_3$	4.60	270	0.317	H \rightarrow L+2 (86%)
	$S_0 \rightarrow S_4$	4.77	260	0.075	H-5 \rightarrow L (31%)

^a Experimental; Absorption energy (λ_{max})= 400 nm

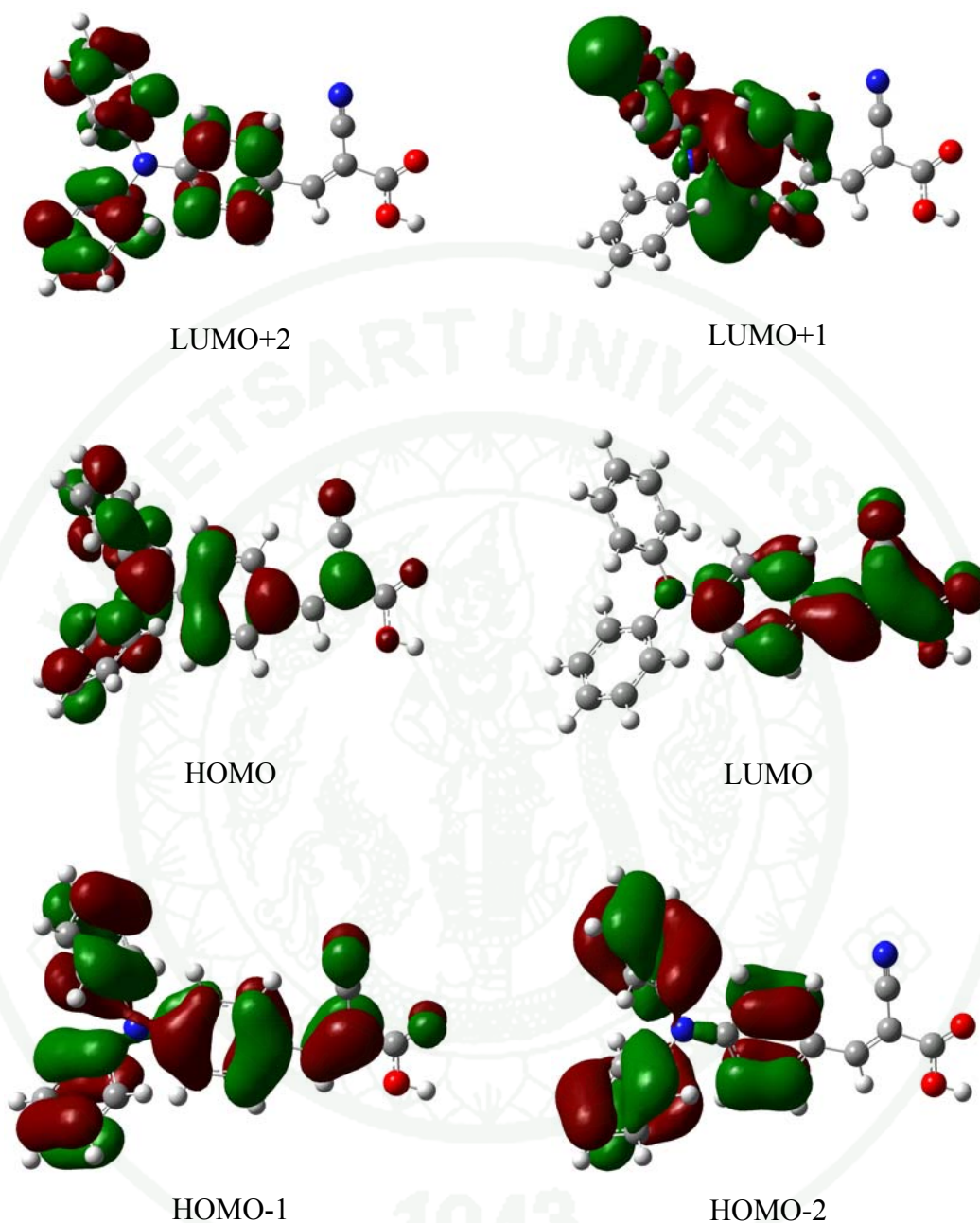


Figure 11 Electronic density of frontier orbitals of TC1 molecule.

To confirm that SS-PCM-TD-CAM-B3LYP is suitable method for predict excitation energies of triphenylamin cyanoacrylic acid and its derivative. The vertical

excitation of TC2, TC3 and TC4 were therefore calculated by SS-PCM-TD-CAM-B3LYP/6-311G(d,p) based on ground state geometries optimization at M06-HF/6-311G(d) level of theory. The vertical excitation of all compound are presented in Table 8.

Table 8 Vertical excitation of triphenylamine cyanoacrylic acid derivative (TC1-TC4) obtained from TD-CAM-B3LYP/6-311G(d,p) that was calculated in SS-PCM methods, compared with maximum absorbance from experimental data^a (E_{xpt}).

Compounds	State	Excitation				Transition
		E_{ex} (eV)	λ_{max} (nm)	E_{xpt} (nm)	f	
TC1	$S_0 \rightarrow S_1$	3.15	393	400	1.197	H \rightarrow L (91%)
	$S_0 \rightarrow S_2$	4.32	287		0.047	H \rightarrow L+1 (81%)
	$S_0 \rightarrow S_3$	4.60	270		0.317	H \rightarrow L+2 (86%)
	$S_0 \rightarrow S_4$	4.77	260		0.075	H-5 \rightarrow L (31%)
TC2	$S_0 \rightarrow S_1$	3.12	397	403	1.289	H \rightarrow L (89%)
	$S_0 \rightarrow S_2$	4.21	295		0.301	H \rightarrow L+1 (76%)
	$S_0 \rightarrow S_3$	4.37	284		0.201	H \rightarrow L+2 (67%)
	$S_0 \rightarrow S_4$	4.70	264		0.076	H \rightarrow L+3 (28%)
TC3	$S_0 \rightarrow S_1$	3.01	412	416	1.503	H \rightarrow L (90%)
	$S_0 \rightarrow S_2$	3.58	346		0.586	H \rightarrow L+1 (84%)
	$S_0 \rightarrow S_3$	4.37	284		0.012	H \rightarrow L+2 (63%)
	$S_0 \rightarrow S_4$	4.59	270		0.007	H-5 \rightarrow L (25%)
TC4	$S_0 \rightarrow S_1$	2.93	423	425	1.618	H \rightarrow L (83%)
	$S_0 \rightarrow S_2$	4.08	304		0.230	H \rightarrow L+1 (74%)
	$S_0 \rightarrow S_3$	4.25	292		0.005	H \rightarrow L+2 (54%)
	$S_0 \rightarrow S_4$	4.30	288		0.541	H-1 \rightarrow L (27%)

Sources: ^a Xu *et al.* (2008)

The maximum absorption wavelength from calculation of TC1, TC2, TC3 and TC4 are 393, 397, 412 and 423 nm, respectively. These wavelengths were compared

with experimental data from Xu *et al.* 2008. The results shown that the maximum absorption wavelength obtained from SS-PCM-TD-CAM-B3LYP of all compounds correspond to experimental data. The main transition of all compounds is corresponded to the excitation from HOMO to LUMO.

Electron density of frontier orbitals for TC2, TC3 and TC4 compounds are presented in Figure 12-14. These electron densities indicate that electron will transfer from triphenylamine group to cyanoacrylic acid group during the excitation from HOMO (ground state) to LUMO (excited state). The different structures of each compound made the different efficiency of electron transfer. The observation of electron transfer between TC1 (shown in Figure 11) and TC4 compounds (shown in Figure 14) indicate that electron transfer of TC4 can transfer from TPA group to cyanoacrylic acid group more than the electron transfer of TC1, due to TC4 compound has added electron donor group and spacer group in the structure. The electron transfer process from TC4 is therefore expected to be more efficiency than that of TC1 compound.

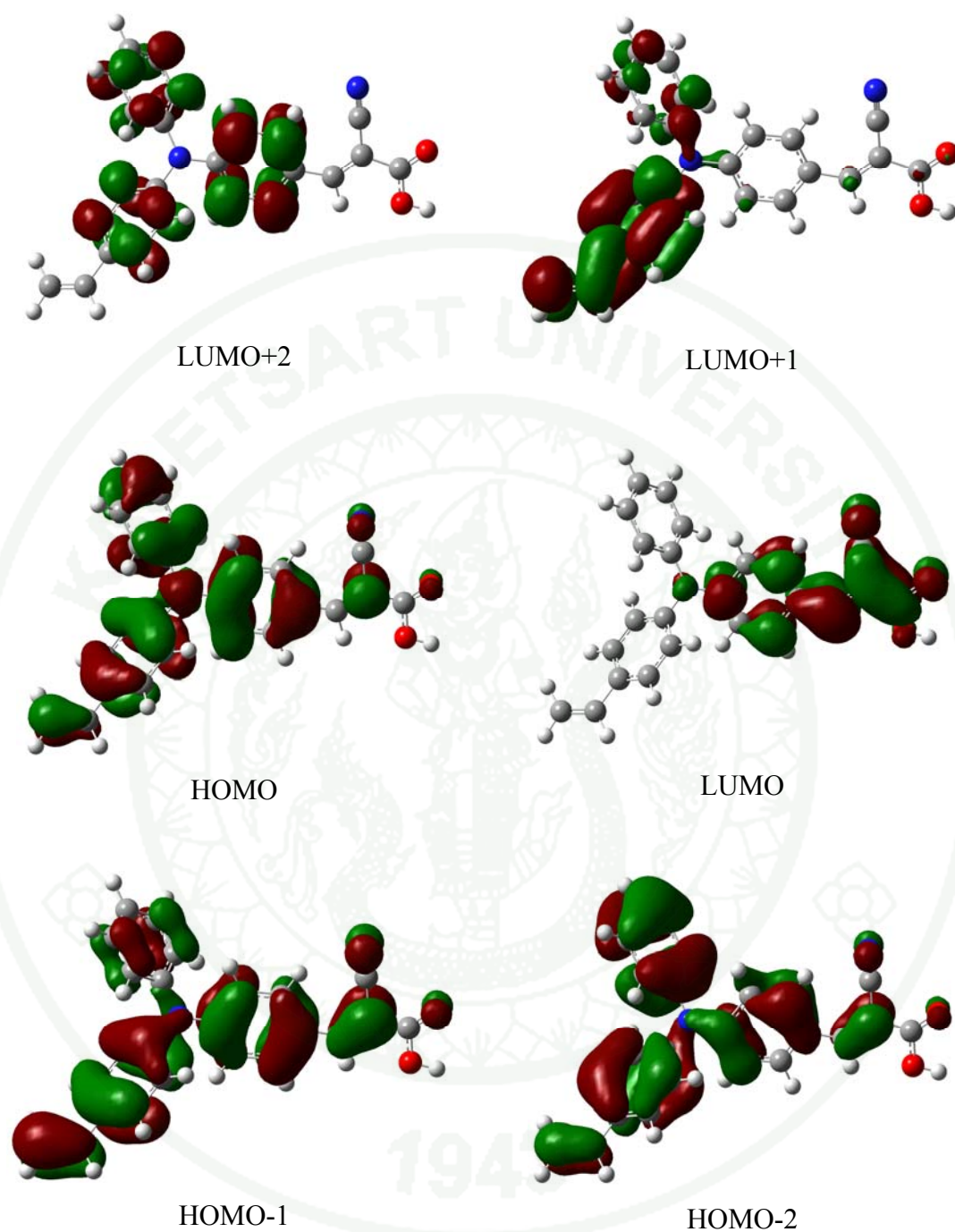


Figure 12 Electronic density of frontier orbitals of TC2 molecule.

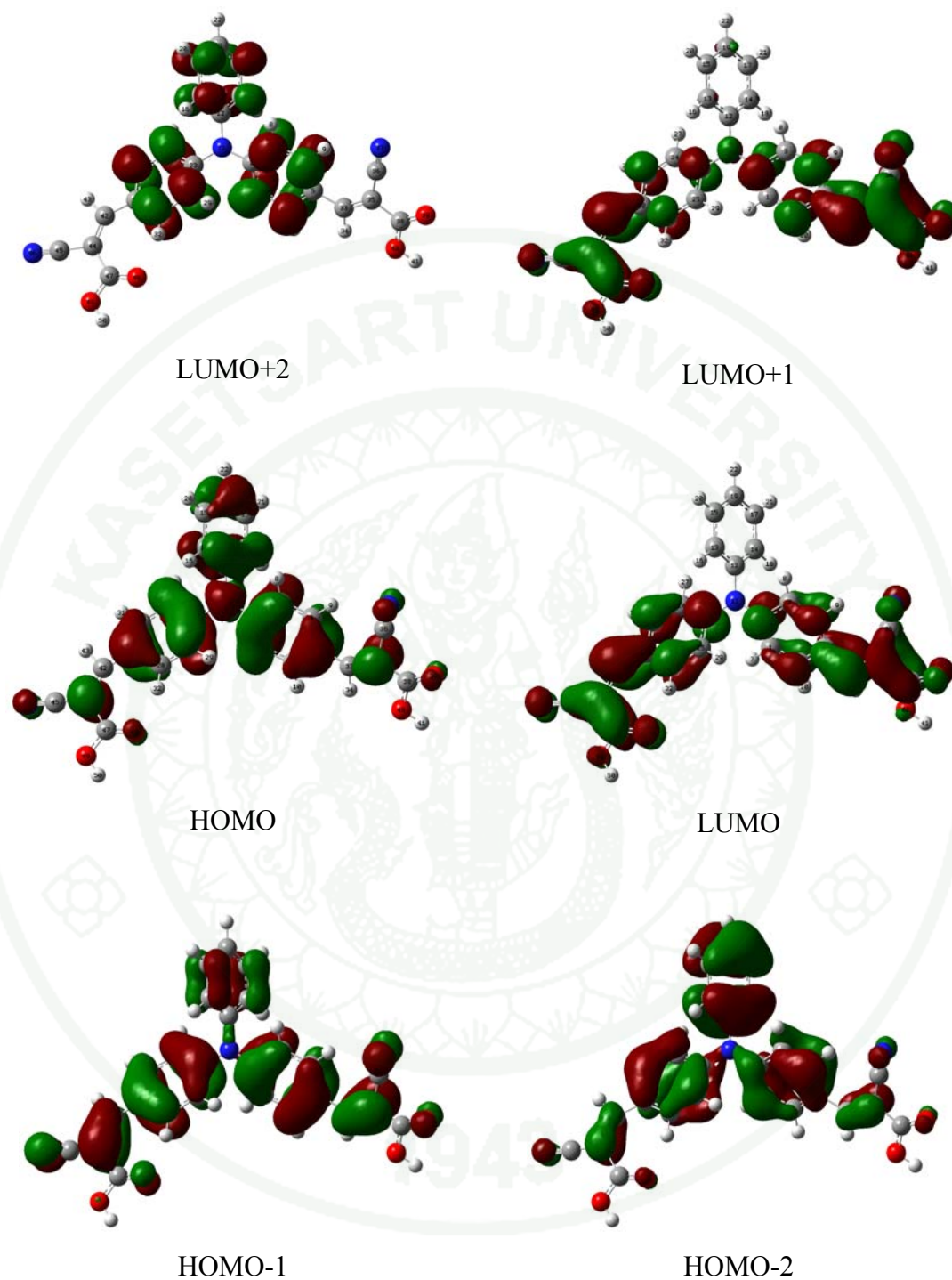
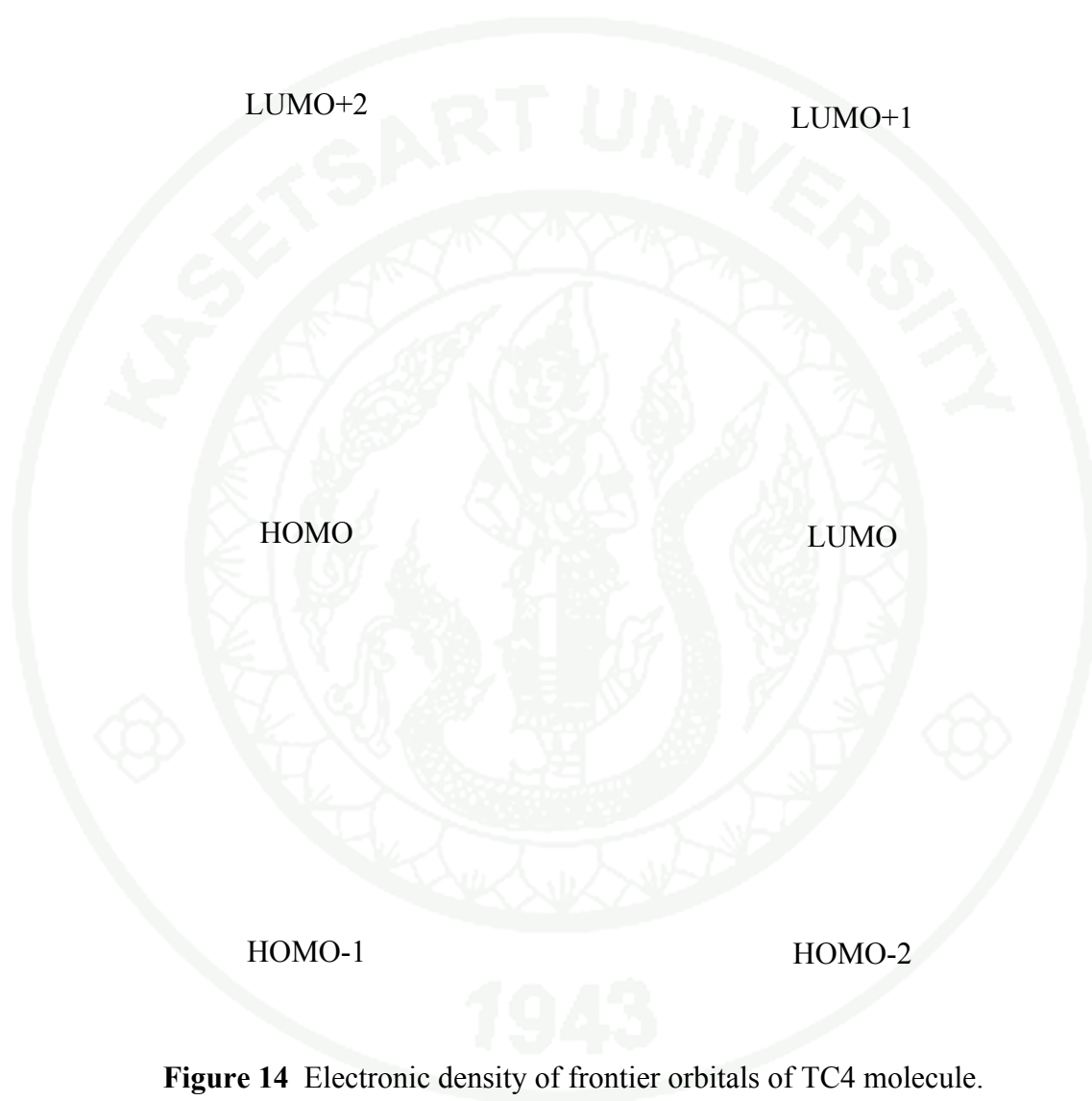


Figure 13 Electronic density of frontier orbitals of TC3 molecule.



4 Efficiency prediction by ionization potential (IP) and electron affinity (EA)

The efficient charge injection is an important parameter for a sensitizer in Dye-sensitized solar cells. The ionization potential (IP) and electron affinity (EA) are used to evaluate the energy barrier for injection of holes and electrons. The calculated results at M06-HF/6-31G(d,p) and percent conversion efficiency from Xu *et al.* (2008) are listed in Table 9. The results in Table 9 shown that TC4 compound has a lowest IP and a higher EA values compared to TC1 compound. This indicates that the adding of electron donating group and electron withdrawing group resulted in the increase in the creation of holes and electrons. The lower IP value of TC4 indicate that the entrance of holes from the conducting transparent oxide to the hole-transport layer was easier compared to TC1. The same analogy was applied for the higher EA value of TC4, where there was an easier entrance of electrons from cathode to the electron-transport layer. These results are well agreement with experimental data. The electron injection process from TC4 is therefore expected to be more efficiency than that of TC1 compound.

Table 9 Ionization potential (IP) and electron affinity (EA), calculated at M06-HF/6-31G(d), compared with percent conversion efficiency (η) from experimental data.

Compounds	IP ^a (eV)	EA ^a (eV)	η ^b /%
TC1	7.26	1.17	2.47
TC2	7.14	1.21	2.86
TC3	7.45	1.47	3.01
TC4	7.02	1.46	4.82

^a Ionization potential (IP), electron affinity (EA)

^b Percents conversion efficiency from Xu *et al.* (2008)

5 Synthesis of 2-cyano-3-(4-(diphenylamino)-phenyl) acrylic acid and absorption properties

The synthesis of 2-cyano-3-(4-(diphenylamino)-phenyl) acrylic acid (TC1) was started by 4-(Diphenylamino)benzaldehyde with cyanoacetic acid as an acetic acid reagents, then reflux in ammonium acetate for 3 hour to give 2-cyano-3-(4-(diphenylamino)-phenyl) acrylic acid (TC1).

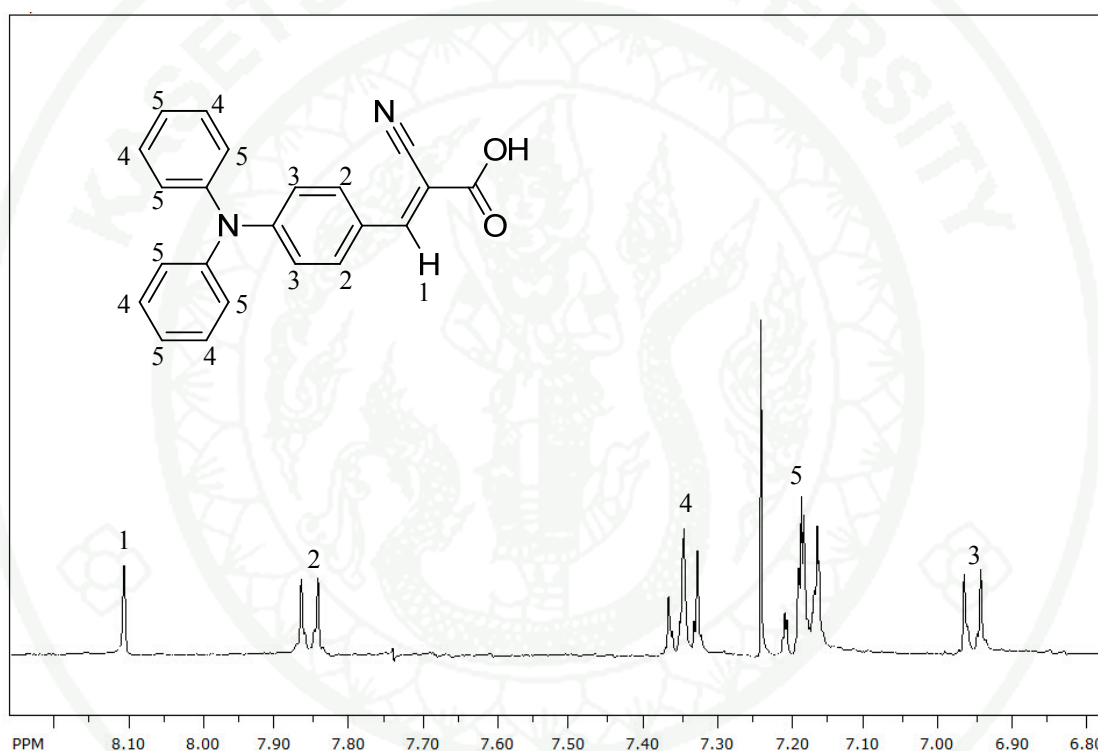


Figure 15 ^1H -NMR spectrum of 2-cyano-3-(4-(diphenylamino)-phenyl) acrylic acid.

The spectrum of ^1H -NMR measurement are shown in Figure 15. The ^1H -NMR spectrum of TC1 was easily obtained because it can be dissolved in d -chloroform (CDCl_3) at room temperature. The ^1H -NMR spectrum exhibits the chemical shift of vinyl group show at 8.1 ppm. The aromatic group (triphenylamine) signal appears at 6.95-7.85 ppm.

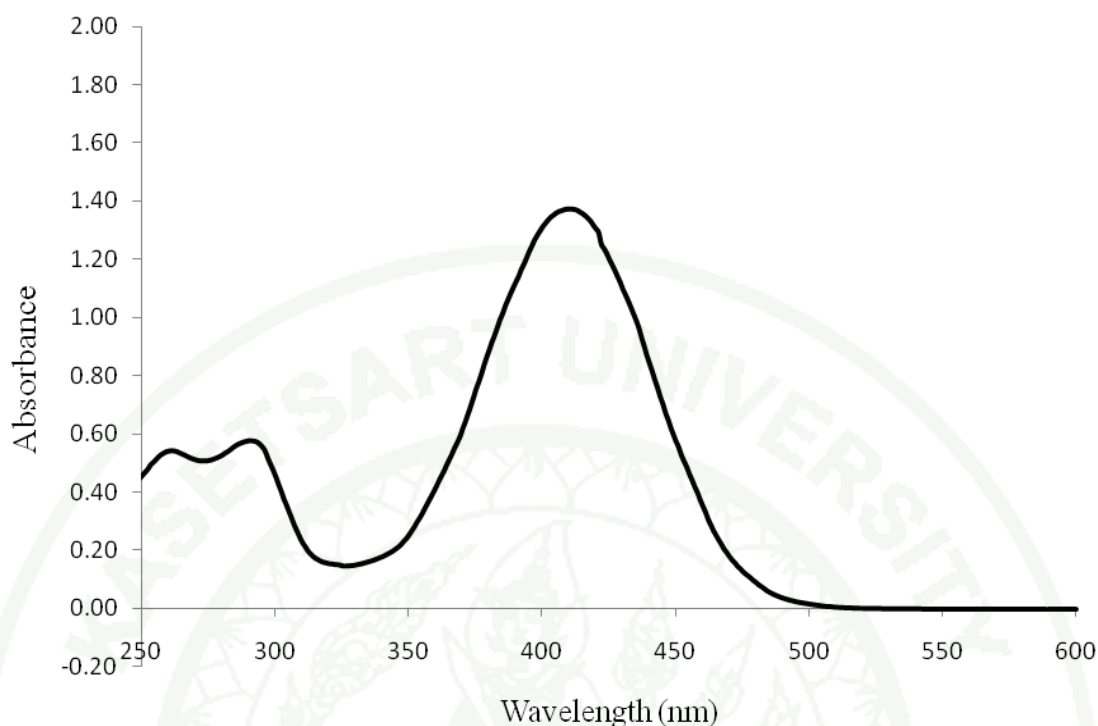


Figure 16 Absorption spectra of 2-cyano-3-(4-(diphenylamino)-phenyl) acrylic acid.

Figure 16 shows the absorption spectra of TC1 in methanol solution, with two distinct absorptions around 300 and 409 nm. The absorption band around 300 nm was assigned to a π - π^* transition, while the absorption band with λ_{max} around 409 nm corresponded to an intramolecular charge transfer (ICT) between the TPA donor part of the molecule and the acceptor end group

CONCLUSION

In this studied, the structures of triphenylamine cyanoacrylic acid and its derivatives were investigated using theoretical studied. The results shown that the absorption band from TD-B3LYP/6-31G(d,p)//M06-HF/6-31G(d) method are in well agreement with experimental data than another method. Therefore, M06-HF/6-31G method was selected to optimize the structure of triphenylamine cyanoacrylic acid and its derivatives.

Furthermore, we have compared the performances of the TD-DFT methods to predict the electronic transition of triphenylaminecyanoacrylic acid (TC1). The results show that the absorption spectrum using the state-specific polarizable continuum model (SS-PCM) TD-CAM-B3LYP/6-311G(d,p) methods) are closer to experimental absorption data. We conclude that the CAM-B3LYP method is reliable method for calculate excitation energies of triphenylamine cyanoacrylic acid and its derivatives

The electronic density of frontier orbitals demonstrate that electron will be transferred from triphenylamine group to cyanoacrylic acid group and then toward to the conduction band of TiO_2 . The results also indicate that the addition of electron donating and spacer groups at triphenylamine, electron transfer will be increased which correspond to the increasing of percent conversion efficiency from experimental data. Moreover, the ionization potential and electron affinity from calculation show that TC4 compound has efficient electron injection TiO_2 which correspond to percent conversion efficiency. This investigation can be exploited in design of novel optical materials for dye-sensitized solar cells.

LITERATURE CITED

- Bonhôte, P., J.-E. Moser, R. Humphry-Baker, N. Vlachopoulos, S.M. Zakeeruddin, L. Walder and M. Grätzel. 1999. Long-Lived Photoinduced Charge Separation and Redox-Type Photochromism on Mesoporous Oxide Films Sensitized by Molecular Dyads. **Journal of the American Chemical Society** 121(6):1324-1336.
- Ehret, A., L. Stuhl and M.T. Spitler. 2001. Spectral Sensitization of TiO₂ Nanocrystalline Electrodes with Aggregated Cyanine Dyes. **The Journal of Physical Chemistry B** 105(41):9960-9965.
- Grätzel, M. 2004. Conversion of sunlight to electric power by nanocrystalline dye-sensitized solar cells. **Journal of Photochemistry and Photobiology A: Chemistry** 164(1-3):3-14.
- Hagberg, D.P., T. Edvinsson, T. Marinado, G. Boschloo, A. Hagfeldt and L. Sun. 2006. A novel organic chromophore for dye-sensitized nanostructured solar cells. **Chemical Communications** (21):2245-2247.
- Hagberg, D.P., T. Marinado, K.M. Karlsson, K. Nonomura, P. Qin, G. Boschloo, T. Brinck, A. Hagfeldt and L. Sun. 2007. Tuning the HOMO and LUMO Energy Levels of Organic Chromophores for Dye Sensitized Solar Cells. **The Journal of Organic Chemistry** 72(25):9550-9556.
- Hagberg, D.P., J.-H. Yum, H. Lee, F. De Angelis, T. Marinado, K.M. Karlsson, R. Humphry-Baker, L. Sun, A. Hagfeldt, M. Grätzel and M.K. Nazeeruddin. 2008. Molecular Engineering of Organic Sensitizers for Dye-Sensitized Solar Cell Applications. **Journal of the American Chemical Society** 130(19):6259-6266.

- Hara, K., T. Sato, R. Katoh, A. Furube, Y. Ohga, A. Shinpo, S. Suga, K. Sayama, H. Sugihara and H. Arakawa. 2002. Molecular Design of Coumarin Dyes for Efficient Dye-Sensitized Solar Cells. **The Journal of Physical Chemistry B** 107(2):597-606.
- Hemalatha, M.R.K. and I. Noorbachta. 1997. An Undergraduate Physical Chemistry Experiment on the Analysis of First-Order Kinetic Data. **Journal of Chemical Education** 74(8):972-null.
- Hwang, S., J.H. Lee, C. Park, H. Lee, C. Kim, C. Park, M.-H. Lee, W. Lee, J. Park, K. Kim, N.-G. Park and C. Kim. 2007. A highly efficient organic sensitizer for dye-sensitized solar cells. **Chemical Communications** (46):4887-4889.
- Justin Thomas, K.R., Y.-C. Hsu, J.T. Lin, K.-M. Lee, K.-C. Ho, C.-H. Lai, Y.-M. Cheng and P.-T. Chou. 2008. 2,3-Disubstituted Thiophene-Based Organic Dyes for Solar Cells. **Chemistry of Materials** 20(5):1830-1840.
- Kitamura, T., M. Ikeda, K. Shigaki, T. Inoue, N.A. Anderson, X. Ai, T. Lian and S. Yanagida. 2004. Phenyl-Conjugated Oligoene Sensitizers for TiO₂ Solar Cells. **Chemistry of Materials** 16(9):1806-1812.
- Li, G., K.-J. Jiang, Y.-F. Li, S.-L. Li and L.-M. Yang. 2008. Efficient Structural Modification of Triphenylamine-Based Organic Dyes for Dye-Sensitized Solar Cells. **The Journal of Physical Chemistry C** 112(30):11591-11599.
- Liang, M., W. Xu, F. Cai, P. Chen, B. Peng, J. Chen and Z. Li. 2007. New Triphenylamine-Based Organic Dyes for Efficient Dye-Sensitized Solar Cells. **The Journal of Physical Chemistry C** 111(11):4465-4472.

Liu, W.-H., I.C. Wu, C.-H. Lai, C.-H. Lai, P.-T. Chou, Y.-T. Li, C.-L. Chen, Y.-Y.

Hsu and Y. Chi. 2008. Simple organic molecules bearing a 3,4-ethylenedioxythiophene linker for efficient dye-sensitized solar cells.

Chemical Communications (41):5152-5154.

Nazeeruddin, M.K., F. De Angelis, S. Fantacci, A. Selloni, G. Viscardi, P. Liska, S.

Ito, B. Takeru and M. Grätzel. 2005. Combined Experimental and DFT-TDDFT Computational Study of Photoelectrochemical Cell Ruthenium Sensitizers. **Journal of the American Chemical Society** 127(48):16835-16847.

Pastore, M., S. Fantacci and F. De Angelis. 2010. Ab Initio Determination of Ground and Excited State Oxidation Potentials of Organic Chromophores for Dye-Sensitized Solar Cells. **The Journal of Physical Chemistry C** 114(51):22742-22750.

Preat, J., C. Michaux, D. Jacquemin and E.A. Perpète. 2009. Enhanced Efficiency of Organic Dye-Sensitized Solar Cells: Triphenylamine Derivatives. **The Journal of Physical Chemistry C** 113(38):16821-16833.

Qin, P., H. Zhu, T. Edvinsson, G. Boschloo, A. Hagfeldt and L. Sun. 2008. Design of an Organic Chromophore for P-Type Dye-Sensitized Solar Cells. **Journal of the American Chemical Society** 130(27):8570-8571.

Robertson, N. 2006. Optimizing Dyes for Dye-Sensitized Solar Cells. **Angewandte Chemie International Edition** 45(15):2338-2345.

Satoh, N., J.-S. Cho, M. Higuchi and K. Yamamoto. 2003. Novel Triarylamine Dendrimers as a Hole-Transport Material with a Controlled Metal-Assembling Function. **Journal of the American Chemical Society** 125(27):8104-8105.

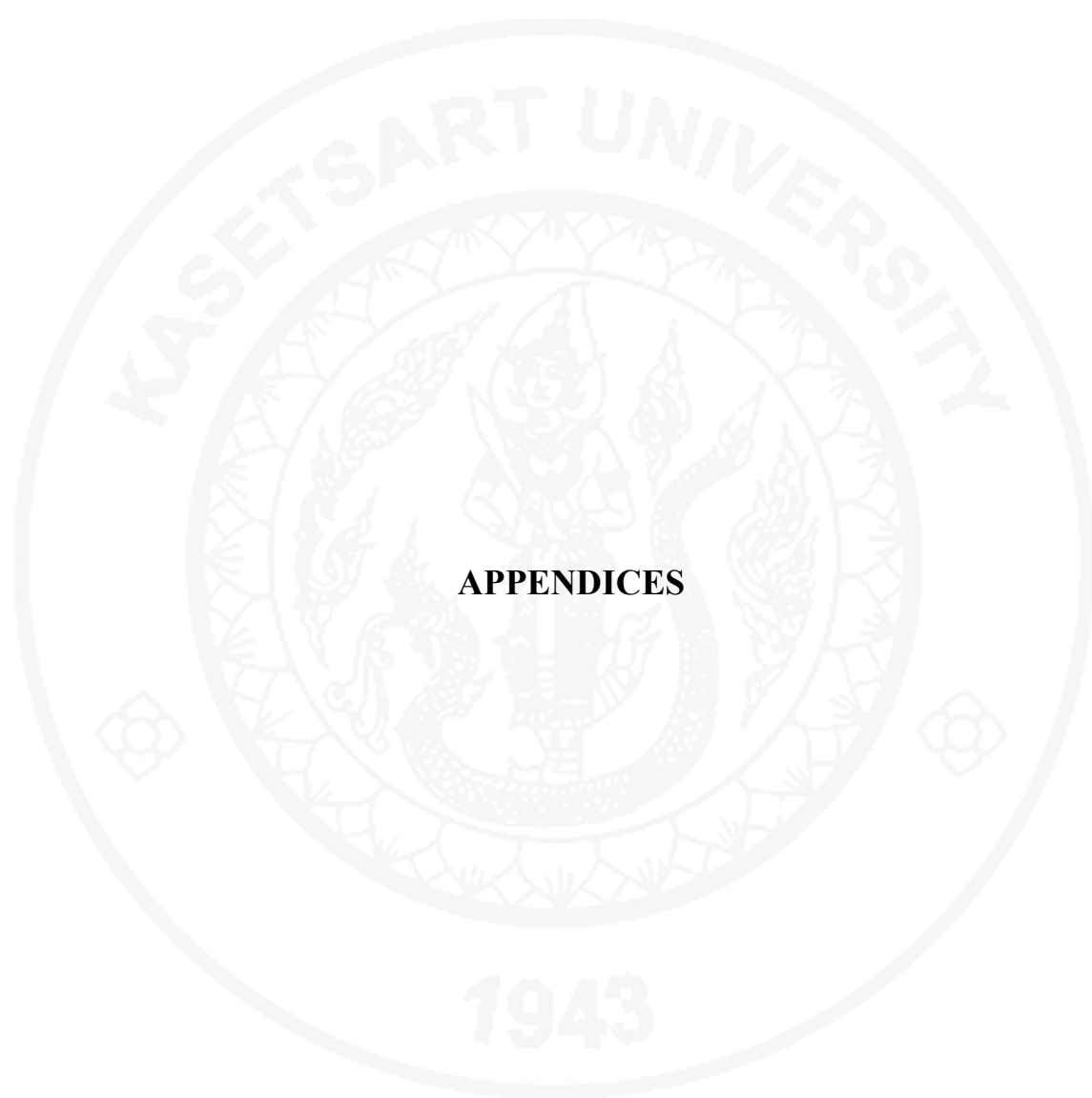
- Satoh, N., T. Nakashima and K. Yamamoto. 2005. Metal-Assembling Dendrimers with a Triarylamine Core and Their Application to a Dye-Sensitized Solar Cell. **Journal of the American Chemical Society** 127(37):13030-13038.
- Sayama, K., S. Tsukagoshi, K. Hara, Y. Ohga, A. Shinpou, Y. Abe, S. Suga and H. Arakawa. 2002. Photoelectrochemical Properties of J Aggregates of Benzothiazole Merocyanine Dyes on a Nanostructured TiO₂ Film. **The Journal of Physical Chemistry B** 106(6):1363-1371.
- Song, J., F. Zhang, C. Li, W. Liu, B. Li, Y. Huang and Z. Bo. 2009. Phenylethyne-Bridged Dyes for Dye-Sensitized Solar Cells. **The Journal of Physical Chemistry C** 113(30):13391-13397.
- Srinivas, K., K. Yesudas, K. Bhanuprakash, V.J. Rao and L. Giribabu. 2009. A Combined Experimental and Computational Investigation of Anthracene Based Sensitizers for DSSC: Comparison of Cyanoacrylic and Malonic Acid Electron Withdrawing Groups Binding onto the TiO₂ Anatase (101) Surface. **The Journal of Physical Chemistry C** 113(46):20117-20126.
- Teng, C., X. Yang, C. Yang, S. Li, M. Cheng, A. Hagfeldt and L. Sun. 2010. Molecular Design of Anthracene-Bridged Metal-Free Organic Dyes for Efficient Dye-Sensitized Solar Cells. **The Journal of Physical Chemistry C** 114(19):9101-9110.
- Velusamy, M., K.R. Justin Thomas, J.T. Lin, Y. C. Hsu and K.C. Ho. 2005. Organic Dyes Incorporating Low-Band-Gap Chromophores for Dye-Sensitized Solar Cells. **Organic Letters** 7(10):1899-1902.
- Wang, Q., S.M. Zakeeruddin, J. Cremer, P. Bäuerle, R. Humphry-Baker and M. Grätzel. 2005. Cross Surface Ambipolar Charge Percolation in Molecular Triads on Mesoscopic Oxide Films. **Journal of the American Chemical Society** 127(15):5706-5713.

Wang, Z.-S., F.-Y. Li, C.H. Huang, L. Wang, M. Wei, L.P. Jin and N.Q. Li. 2000. Photoelectric Conversion Properties of Nanocrystalline TiO₂ Electrodes Sensitized with Hemicyanine Derivatives. **The Journal of Physical Chemistry B** 104(41):9676-9682.

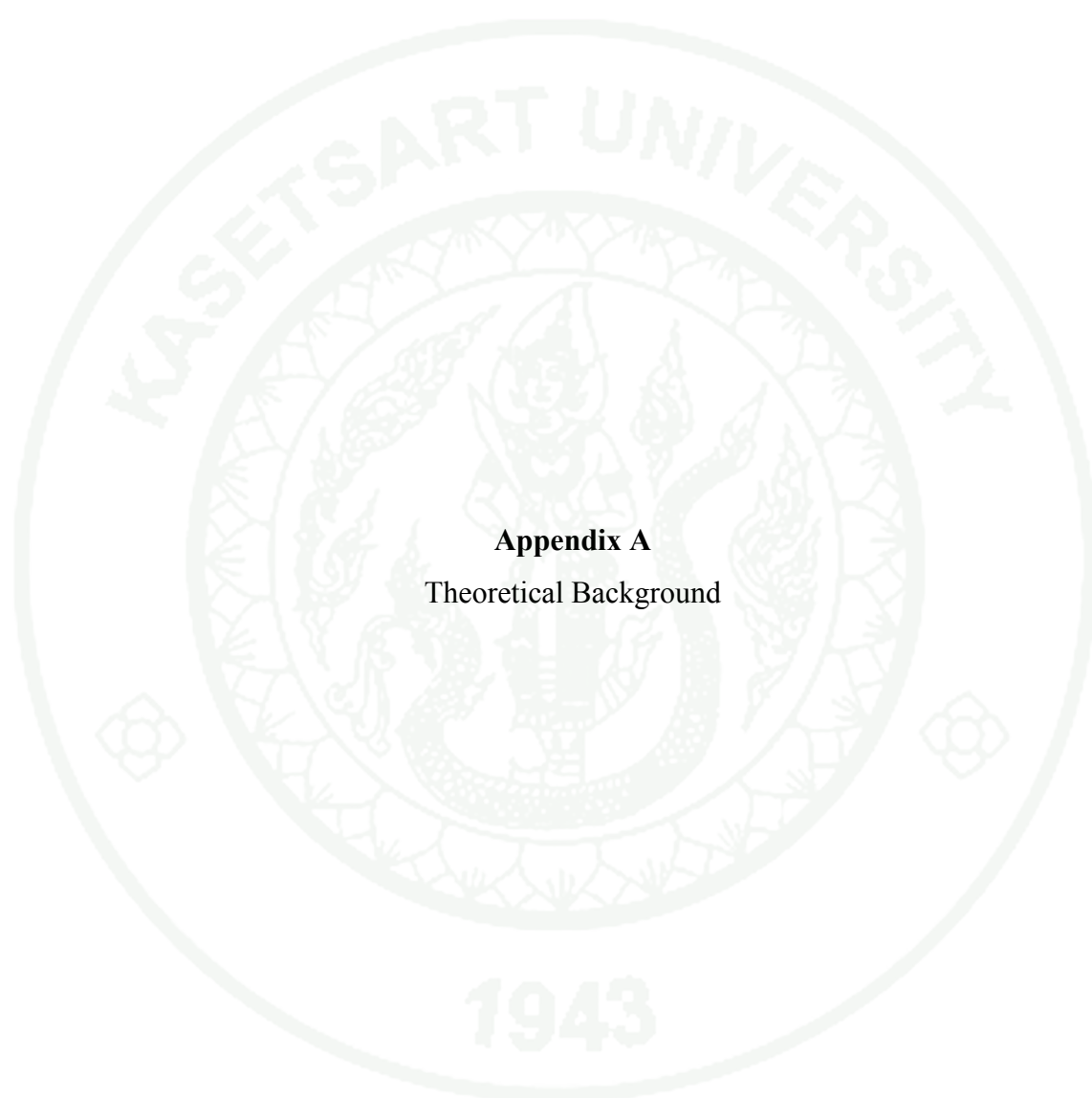
Xu, W., B. Peng, J. Chen, M. Liang and F. Cai. 2008. New Triphenylamine-Basedd Dyes for Dye-Sensitized Solar Cells. **The Journal of Physical Chemistry C** 112(3):874-880.

Yang, C.H., H.L. Chen, Y.Y. Chuang, C.G. Wu, C.P. Chen, S.H. Liao and T.L. Wang. 2009. Characteristics of triphenylamine-basedd dyes with multiple acceptors in application of dye-sensitized solar cells. **Journal of Power Sources** 188(2):627-634.

Zhang, W., Z. Fang, M. Su, M. Saeys and B. Liu. 2009. A Triphenylamine-Basedd Conjugated Polymer with Donor- π -Acceptor Architecture as Organic Sensitizer for Dye-Sensitized Solar Cells. **Macromolecular Rapid Communications** 30(18):1533-1537.



APPENDICES

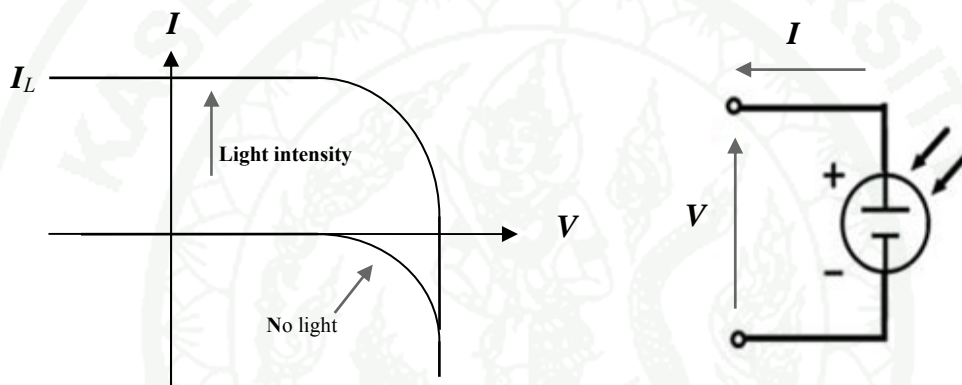


Appendix A
Theoretical Background

Solar Cells Parameter

1.1 Theory of I-V Characterization

PV cells can be modeled as a current source in parallel with a diode. When there is no light present to generate any current, the PV cell behaves like a diode. As the intensity of incident light increases, current is generated by the PV cell, as illustrated in Figure A1.



Appendix Figure A1 I-V curve of PV cell and associated electrical diagram.

In an ideal cell, the total current I is equal to the current I_L generated by the photoelectric effect minus the diode current I_D , according to the equation 1.

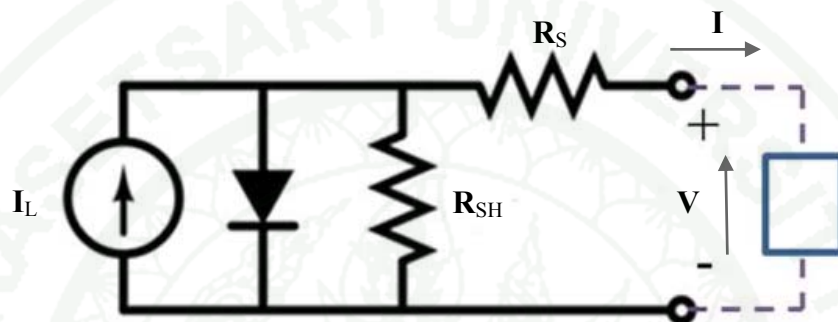
$$I = I_L - I_D = I_L - I_0 \left(e^{\frac{qV}{kT}} - 1 \right) \quad (1)$$

where I_0 is the saturation current of the diode, q is the elementary charge 1.6×10^{-19} Coulombs, k is a constant of value 1.38×10^{-23} J/K, T is the cell temperature in Kelvin, and V is the measured cell voltage that is either produced (power quadrant) or applied (voltage bias). A more accurate model will include two diode terms; however, we will concentrate on a single diode model in this document.

Expanding the equation gives the simplified circuit model shown below and the following associated equation, where n is the diode ideality factor (typically

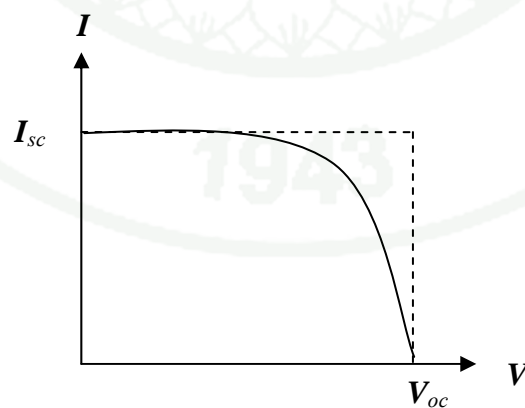
between 1 and 2), and R_S and R_{SH} represents the series and shunt resistances that are described in further detail later in figure A2

$$I = I_L - I_0 \left(e^{\frac{q(V+I \cdot R_S)}{n \cdot k \cdot T}} - 1 \right) - \frac{V + I \cdot R_S}{R_{SH}} \quad (2)$$



Appendix Figure A2 Simplified equivalent circuit model for a photovoltaic cell.

The I - V curve of an illuminated PV cell has the shape shown in Figure A3 as the voltage across the measuring load is swept from zero to V_{OC} , and many performance parameters for the cell can be determined from this data, as described in the sections below.



Appendix Figure A3 Illuminated I-V sweep curve.

1.2 Power Conversion Efficiency

The power conversion efficiency is ratio of electrical power output (P_{out}), compared to the solar power input (P_{in}) into the PV cell. P_{out} can be taken to be P_{MAX} since the solar cell can be operated up to its maximum power output to get the maximum efficiency. The solar energy-to-electricity conversion efficiency (η) of DSSC is defined by the following equation 2.

$$\eta = \frac{P_{out}}{P_{in}} = \frac{I_{sc} V_{oc} FF}{P_{in}} \times 100 \quad (3)$$

Where P_{in} is taken as the product of the irradiance of the incident light, measured in W/m² or in suns (1000 W/m²), with the surface area of the solar cell (m²) I_{sc} is the short-circuit current density under irradiation, V_{oc} is the open-circuit voltage, FF is the fill factor.

1.3 Short Circuit Current (I_{sc})

The short circuit current I_{sc} corresponds to the short circuit condition when the impedance is low and is calculated when the voltage equals zero.

$$I_{(at\ V=0)} = I_{sc} \quad (4)$$

I_{sc} occurs at the beginning of the forward-bias sweep and is the maximum current value in the power quadrant. For an ideal cell, this maximum current value is the total current produced in the solar cell by photon excitation.

The short-circuit current is due to the generation and collection of light-generated carriers. For an ideal solar cell at most moderate resistive loss mechanisms, the short-circuit current and the light-generated current are identical. Therefore, the short-circuit current is the largest current which may be drawn from the solar cell.

1.4 Open Circuit Voltage (V_{oc})

The open circuit voltage (V_{oc}) occurs when there is no current passing through the cell.

$$V_{(at\ I=0)} = V_{oc} \quad (5)$$

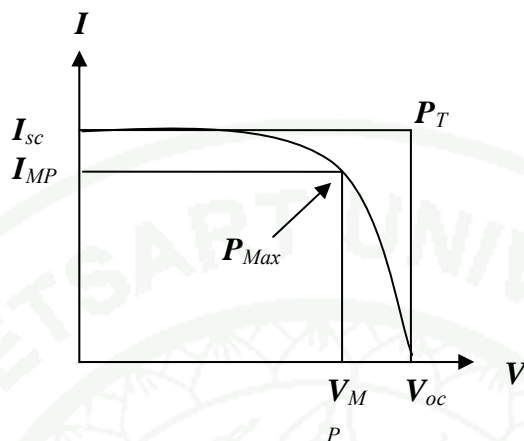
The open-circuit voltage corresponds to the amount of forward bias on the solar cell due to the bias of the solar cell junction with the light-generated current.

1.5 Maximum Power (P_{MAX}), Current at P_{MAX} (I_{MP}), Voltage at P_{MAX} (V_{MP})

The power produced by the cell in Watts can be easily calculated along the I - V sweep by the equation $P=IV$. At the ISC and V_{oc} points, the power will be zero and the maximum value for power will occur between the two. The voltage and current at this maximum power point are denoted as V_{MP} and I_{MP} respectively.

1.6 Fill Factor (FF)

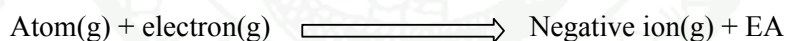
The Fill Factor (FF) is essentially a measure of quality of the solar cell. It is calculated by comparing the maximum power to the theoretical power (P_T) that would be output at both the open circuit voltage and short circuit current together. FF can also be interpreted graphically as the ratio of the rectangular areas depicted in Figure A4.



Appendix Figure A4 Getting the fill factor from the I - V sweep.

1.7 Electron Affinity (EA)

The Electron affinity (EA) of a molecule or atom is the energy change when an electron is added to the neutral atom to form a negative ion. This property can only be measured in an atom in gaseous state.



- If atom or molecule have high electron affinity, which mean it is easy to accept electron.
- If atom or molecule have low electron affinity, which means it is hard to accept electron.

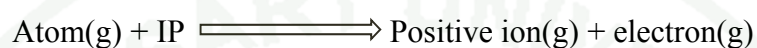
Therefore, we can calculate electron affinity from equation 6

$$E_{EA} = E_{\text{natural}} - E_{\text{negative ion}} \quad (6)$$

Where E is total energy of molecules

1.8 Ionization Potential (IP)

The Ionization potential (IP) is the amount of energy required to remove one or more electrons from the outermost shell of an isolated atom in the gaseous state.



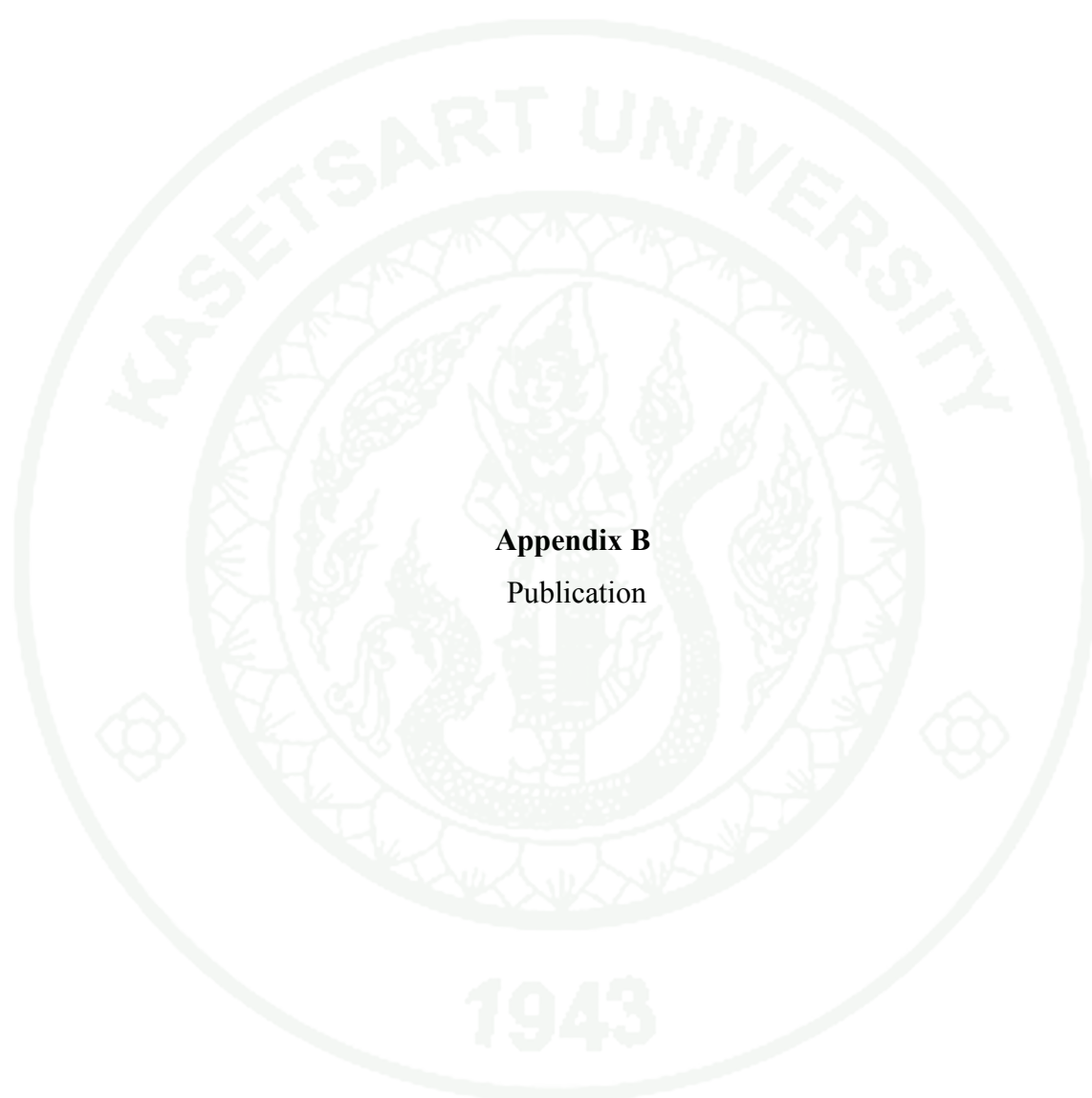
- If atom or molecules have high ionization potential, which mean it takes a lot of energy to remove the outermost electron.
- If atom or molecules have low ionization potential, which means it takes only a small amount of energy to remove the outermost electron.

Therefore, we can calculate Ionization potential from equation 7

$$E_{EA} = E_{\text{natural}} - E_{\text{positive ion}} \quad (7)$$

Where E is total energy of molecules

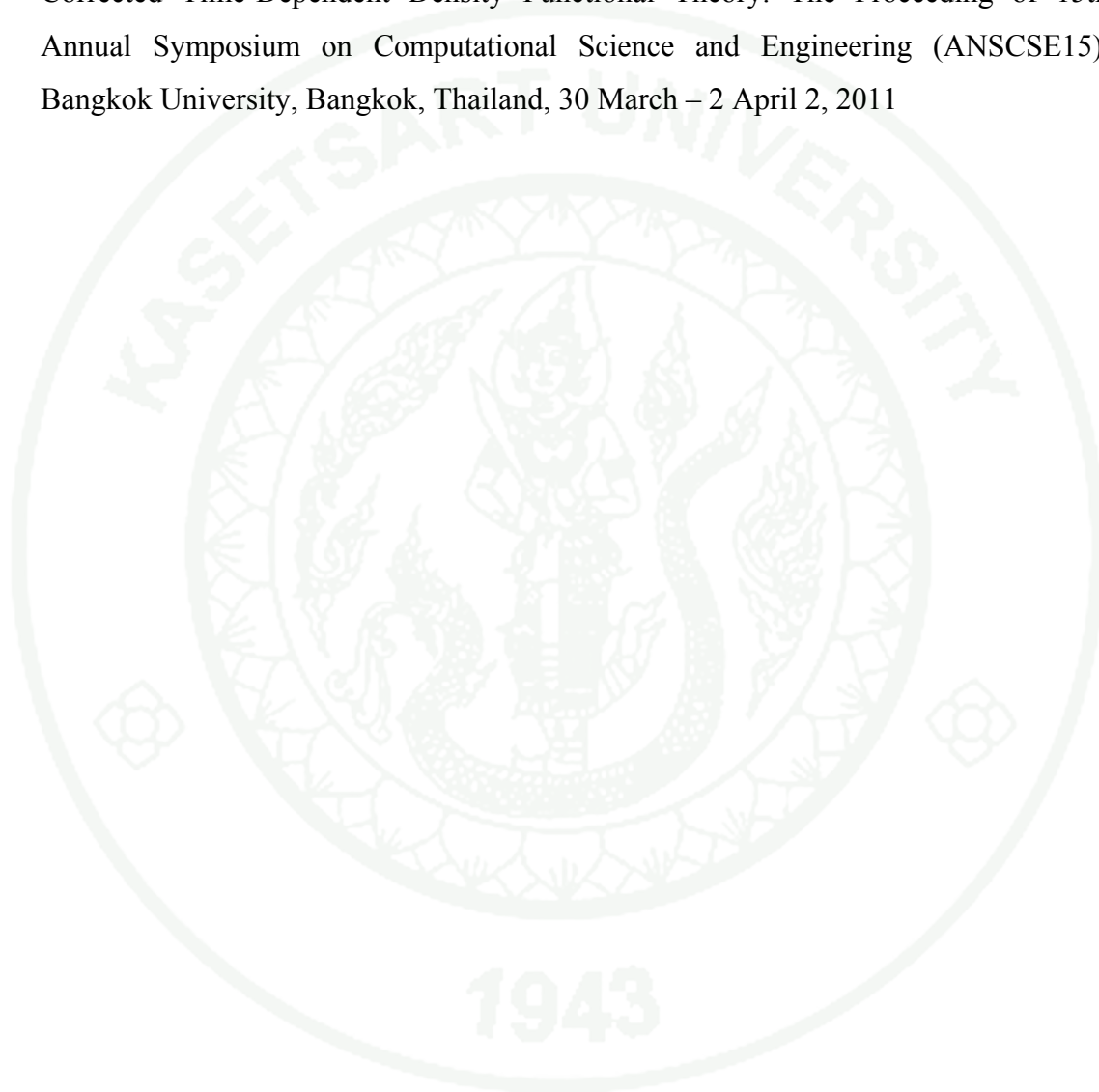




Appendix B
Publication

Publication

Chirawat Chitpakdee, Songwut Suramitr, Supa Hannongbua. Excitation Energies of Triphenylamine Cyanoacrylic Acid for Dye-Sensitized Solar Cells Using Long-Range Corrected Time-Dependent Density Functional Theory. The Proceeding of 15th Annual Symposium on Computational Science and Engineering (ANSCSE15). Bangkok University, Bangkok, Thailand, 30 March – 2 April 2, 2011



Excitation Energies of Triphenylamine Cyanoacrylic Acid for Dye-Sensitized Solar Cells Using Long-Range Corrected Time-Dependent Density Functional Theory

C. Chitpakdee^{1,2}, S. Suramitr^{1,2*} and S. Hannongbua^{1,2}

¹Department of Chemistry, Faculty of Science, Kasetsart University, Bangkok 10900, Thailand

²The Center of Nanotechnology KU, Kasetsart University, Bangkok 10900, Thailand.

*E-mail: fsciswsm@ku.ac.th; Fax: 02-562-5555 ext. 2176; Tel. 02-562-5555 ext. 2227

ABSTRACT

Structures of 2-cyano-3-(4-(diphenylamino)-phenyl) acrylic acid (TC1) was investigated using density functional theory (DFT). The structural parameters were optimized using DFT functional, M06-HF at 6-31G(d) basis set level. The excitation energy were calculated by solutions using long-range corrected time-dependent density functional theory (TD-DFT), PBE0, LC-B3LYP, LC-wPBE, CAM-B3LYP at 6-311G(d,p) level including conductor polarizable continuum model (PCM) solvation to compare with the experimental absorption bands. The results show that the absorption spectrum using the state-specific polarizable continuum model SS-PCM-TD-CAM-B3LYP/6-311G(d,p) methods (393 nm) are closer to experimental absorption data (400 nm). We conclude by discussing the benefits of theoretical calculations, which can provide critical structural and electronic understanding of electron transfer phenomena that can be exploited in design of novel optical materials.

Keywords: Triphenylamine Cyanoacrylic Acid Derivatives, Quantum Chemical Calculation, DFT

1. INTRODUCTION

The dye-sensitized solar cells (DSSCs) have attracted a lot of interest for their abilities to convert solar light to electricity at low cost. The metal-organic dye base on ruthenium sensitizer has shown very impressive solar-to-electric power conversion efficiencies, reaching 11% at standard AM 1.5 sun light [1,2]. Although Ru complexes are suitable as photosensitizers, the limited availability and environmental issues would limit their extensive application. In the meantime, alternative metal-free organic dyes exhibit high molar extinction coefficients and are easily modified due to short synthetic and economically, have shown the conversion efficiencies up to 8% [3-6]. Among the metal free organic dyes, triphenylamine (TPA) and its derivatives as donor units have displayed promising properties in the development of photovoltaic devices [6-8].

Xu's and coworker [9] shown that triphenylamine moieties and a cyanoacetic acid moiety are desirable units in the design of dyes as electron donor and electron acceptor/anchoring group, respectively. Bridge groups, as electron spacers to connect the donor and acceptor, are not only to decide light absorption regions of the DSSCs but also influence the electron injection from excited dyes to the TiO₂ surface.

ANSCSE15 Bangkok University, Thailand
March 30-April 2, 2011

It is interesting about the effective of electron donor and electron acceptor/anchoring group for increase the effectively of DSSC. Accordingly, we have thus focused our investigation using theoretical study with the goal of using density functional theory (DFT) to understand and development of new sensitizers base on triphenylamine (TPA) moieties as the donor and cyanoacetic acid moieties as the electron acceptor groups for solar cell applications. The quantum chemical calculations are the most appropriate alternative for understands the structure and electronic properties of molecules. Their absorption spectra in solvent phase were calculated by time-dependent density functional theory (TD-DFT) and several Polarizable Continuum Model (PCM-TDDFT) approaches.

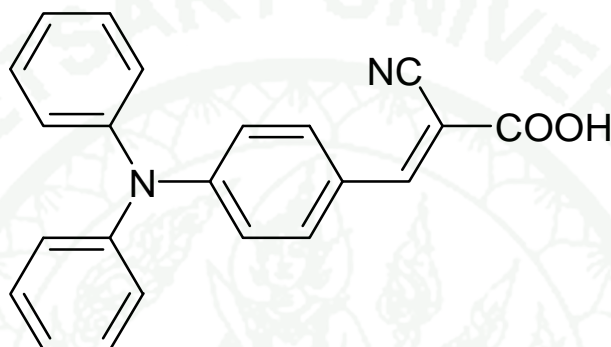


Figure 1. Molecular Structures of triphenylamine-cyanoacrylic acid (TC1).

2. COMPUTATIONAL DETAILS

The geometrical and electronic properties of Triphenylamine-cyanoacrylic acid (TC1) was performed with the Gaussian 09 program package. The structures were optimized using density functional theory (DFT) with M06-HF together with 6-31G(d,p) basis set. The excitation energies were calculated using several TD-DFT functional, PBE0, LC-B3LYP, LC-wPBE, CAM-B3LYP at 6-311G(d,p) level of theory including conductor polarizable continuum model (PCM) solvation based on the optimized structures obtained from M06HF/6-31G(d) method. We study the low-lying excited states of all molecules in various solutions using long-range corrected TDDFT.

The solvation effect on transition energies has been evaluated by means of the PCM approach. The dielectric constant of methanol ($\epsilon = 32.613$) was used in accordance with the measurement of the UV-vis spectra. For absorption, geometry optimization of the S_0 state was performed with equilibrium approach and the PCM-TD-DFT calculations were performed with non-equilibrium scheme. Bulk solvent effect on the excited state was calculated with the linear-response (LR) and state-specific (SS) solvation approach. The results from calculations were compared with the experimental data from Xu's and coworker [9].

3. RESULTS AND DISCUSSION

In the present study, we have investigated the electronic structures and absorption properties of triphenylamine cyanoacrylic acid (TC1) using quantum chemistry calculation. The electronic transition and absorption properties were calculated using TD-DFT calculations base on ground state geometries with various methods including conductor polarizable continuum model salvation in methanol. The computed vertical excitation energies for singlet excited states, together with the oscillator strength and maximum absorbance calculated using different functionals, compared to experimental results are shown

ANSCSE15 Bangkok University, Thailand
March 30-April 2 , 2011

in Table 1. The maximum absorbance using LR-PCM-TD-CAM-B3LYP/6-311G(d,p) methods at 375 nm are in better agreement with the experimental results at 400 nm [9] than the other LR-PCM-TD-DFT functional, PBE0 (429 eV), LC-B3LYP (335 eV) and LC-wPBE (340 eV).

Table 1. Vertical excitation of TC1 molecule obtained from PCM-TD-DFT methods in methanol at 6-311G(d,p) basis set base on ground state geometries and experiment data^a.

Methods	States	E _{ex} (eV)	λ_{\max} (nm)	<i>f</i>	Transition
PBE0	S ₀ →S ₁	2.89	429	0.8390	HOMO→LUMO (99%)
	S ₀ →S ₂	3.98	312	0.0234	HOMO→L+1 (90%)
	S ₀ →S ₃	4.28	290	0.1752	HOMO→L+2 (94%)
	S ₀ →S ₄	4.36	284	0.1549	H-1→LUMO (92%)
LC-BLYP	S ₀ →S ₁	3.71	335	1.1041	HOMO→LUMO (80%)
	S ₀ →S ₂	4.73	262	0.0223	HOMO→L+1 (62%)
	S ₀ →S ₃	5.06	245	0.2413	HOMO→L+2 (76%)
	S ₀ →S ₄	5.17	240	0.0184	HOMO→L+4 (22%)
LC-wPBE	S ₀ →S ₁	3.65	340	1.0928	HOMO→LUMO (81%)
	S ₀ →S ₂	4.66	266	0.0217	HOMO→L+1 (64%)
	S ₀ →S ₃	4.99	249	0.2470	HOMO→L+2 (76%)
	S ₀ →S ₄	5.11	243	0.0178	HOMO→L+4 (25%)
CAM-B3LYP	S ₀ →S ₁	3.31	375	1.0055	HOMO→LUMO (92%)
	S ₀ →S ₂	4.34	286	0.0252	HOMO→L+1 (78%)
	S ₀ →S ₃	4.66	266	0.2136	HOMO→L+2 (86%)
	S ₀ →S ₄	4.80	258	0.0248	H-5→LUMO (33%)

^aExperimental; Absorption energy (λ_{\max})= 400 nm

The results of the low-lying dipole-allowed excited states obtained by different PCM methods of calculation, TD-CAM-B3LYP functional at 6-311G(d,p) basis set are presented in Table 2 for the TC1 molecule. The vertical excitation energies in solution, methanol, are also evaluated within the PCM approach. In the PCM, the equilibrium linear response (LR-PCM-TD-DFT) and state-specific (SS-PCM-TD-DFT) approaches were performed and also compared with the vertical excitation energies in gas phase. The maximum absorbance in gas phase was increased from 354 nm to 375 and 393 nm for calculating by LR-PCM and SS-PCM approaches, respectively. The result shown that the vertical excitation energies were improved when we applied the state specific (SS) in PCM method and are close with experimental data (400 nm).

The assignments of all peaks are almost identical to those of the TD-CAM-B3LYP calculations. The first peak was assigned to the transition from HOMO to LUMO and the second peak, was ascribed to the linear combination of HOMO→LUMO+2 components. All of these states are assigned to the $\pi \rightarrow \pi^*$ transition. The relevant MOs for these transitions are shown in Fig. 2. Figure 2 shows the electronic density of frontier orbitals of TC1. Observation of the frontier orbitals of the dyes shows that the HOMO of TC1 is delocalized over the entire molecule. Simultaneously, the LUMO of both are still delocalized over the entire molecule. Nevertheless, the LUMO of both are mainly delocalized over the cyanoacrylic group

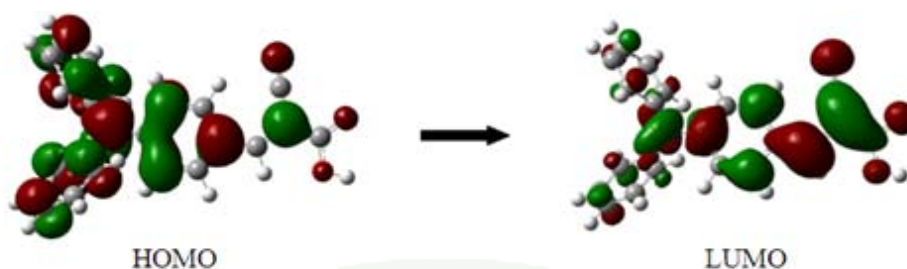


Figure 2. The electronic density of frontier orbitals of TC1 molecule that obtained from SS-PCM-TD-CAMB3LYP/6-311G(d,p)

Table 2. Vertical excitation of TC1 molecule obtained from TD-CAMB3LYP/6-311G(d,p) that was calculated in gas phase and various PCM methods

Methods	States	Eex (eV)	λ_{\max} (nm)	f	Transition
Gas	$S_0 \rightarrow S_1$	3.51	354	0.9077	HOMO \rightarrow LUMO (92%)
	$S_0 \rightarrow S_2$	4.33	286	0.0243	HOMO \rightarrow L+1 (81%)
	$S_0 \rightarrow S_3$	4.64	267	0.1724	HOMO \rightarrow L+2 (89%)
	$S_0 \rightarrow S_4$	4.82	257	0.0137	HOMO \rightarrow L+5 (20%)
LR-PCM	$S_0 \rightarrow S_1$	3.31	375	1.0055	HOMO \rightarrow LUMO (92%)
	$S_0 \rightarrow S_2$	4.34	286	0.0252	HOMO \rightarrow L+1 (78%)
	$S_0 \rightarrow S_3$	4.66	266	0.2136	HOMO \rightarrow L+2 (86%)
	$S_0 \rightarrow S_4$	4.80	258	0.0248	H-5 \rightarrow LUMO (33%)
SS-PCM	$S_0 \rightarrow S_1$	3.15	393	1.1968	HOMO \rightarrow LUMO (91%)
	$S_0 \rightarrow S_2$	4.32	287	0.0467	HOMO \rightarrow L+1 (81%)
	$S_0 \rightarrow S_3$	4.60	270	0.3166	HOMO \rightarrow L+2 (86%)
	$S_0 \rightarrow S_4$	4.77	260	0.0748	H-5 \rightarrow LUMO (31%)
Experiment		3.10	400		

4. CONCLUSIONS

In this studied, we have compared the performances of the TD-DFT methods to predicting the electronic transition of triphenylamine cyanoacrylic acid (TC1). The results show that the absorption spectrum using the state-specific polarizable continuum model (SS-PCM) TD-CAM-B3LYP/6-311G(d,p) methods) are closer to experimental absorption data. We conclude that the CAM-B3LYP method is reliable method for calculate excitation energies of triphenylamine cyanoacrylic acid and its derivatives which that can be exploited in design of novel optical materials for dye- sensitized solar cells.

ACKNOWLEDGMENTS

This work has been supported in part by grants from the National Center of Excellence in Petroleum, Petrochemical Technology, Center of Nanotechnology Kasetsart University, Kasetsart University Research and Development Institute (KURDI),

ANSCSE15 Bangkok University, Thailand
March 30-April 2 , 2011

Laboratory of Computational and Applied Chemistry (LCAC), the Commission on Higher Education via the "National Research University Project of Thailand" (NRU)

REFERENCES

1. Grätzel, M. *Journal of Photochemistry and Photobiology A: Chemistry* **2004**, *164*, 3-14.
2. Nazeeruddin, M. K.; De Angelis, F.; Fantacci, S.; Selloni, A.; Viscardi, G.; Liska, P.; Ito, S.; Takeru, B.; Grätzel, M. *Journal of the American Chemical Society* **2005**, *127*, 16835-16847.
3. Ehret, A.; Stuhl, L.; Spitler, M. T. *The Journal of Physical Chemistry B* **2001**, *105*, 9960-9965.
4. Hara, K.; Sato, T.; Katoh, R.; Furube, A.; Ohga, Y.; Shinpo, A.; Suga, S.; Sayama, K.; Sugihara, H.; Arakawa, H. *The Journal of Physical Chemistry B* **2002**, *107*, 597-606.
5. Sayama, K.; Tsukagoshi, S.; Hara, K.; Ohga, Y.; Shinpo, A.; Abe, Y.; Suga, S.; Arakawa, H. *The Journal of Physical Chemistry B* **2002**, *106*, 1363-1371.
6. Wang, Z.-S.; Li, F.-Y.; Huang, C.-H.; Wang, L.; Wei, M.; Jin, L.-P.; Li, N.-Q. *The Journal of Physical Chemistry B* **2000**, *104*, 9676-9682.
7. Satoh, N.; Cho, J.-S.; Higuchi, M.; Yamamoto, K. *Journal of the American Chemical Society* **2003**, *125*, 8104-8105.
8. Satoh, N.; Nakashima, T.; Yamamoto, K. *Journal of the American Chemical Society* **2005**, *127*, 13030-13038.
9. Xu, W.; Peng, B.; Chen, J.; Liang, M.; Cai, F. *The Journal of Physical Chemistry C* **2008**, *112*, 874-880.

CURRICULUM VITAE

NAME : Mr. Chirawat Chitpakdee

BIRTH DATE : December 08, 1986

BIRTH PLACE : Sisaket, THAILAND

EDUCATION	: <u>YEAR</u>	<u>INSTITUTION</u>	<u>DEGREE/DIPLOMA</u>
	2008	Ubonratchathani University	B.Sc. (Chemistry)

POSITION/TITLE : Postgraduates student

WORKPLACE : Faculty of Science, Kasetsart University

PUBLICATION : Chitpakdee, C., S. Suramitr and S. Hannongbua, Excitation Energies of Triphenylamine Cyanoacrylic Acid for Dye-Sensitized Solar Cells Using Long-Range Corrected Time-Dependent Density Functional Theory, The 15th Annual Symposium on Computational Science and Engineering(ANSCSE15), Bangkok University, Bangkok, Thailand, March 30-April 2, 2011